Annu. Rev. Astron. Astrophys. 2003. 41:57–115
doi: 10.1146/annurev.astro.41.011802.094844

EMBEDDED CLUSTERS IN MOLECULAR CLOUDS

Charles J. Lada
Harvard-Smithsonian Center for Astrophysics, Cambridge, Massachusetts 02138; email: clada@cfa.harvard.edu

Elizabeth A. Lada
Department of Astronomy, University of Florida, Gainesville, Florida 32611; email: lada@astro.ufl.edu

Key Words clusters, star formation, initial mass function, circumstellar disks, brown dwarfs

■ **Abstract** Stellar clusters are born embedded within giant molecular clouds (GMCs) and during their formation and early evolution are often only visible at infrared wavelengths, being heavily obscured by dust. Over the past 15 years advances in infrared detection capabilities have enabled the first systematic studies of embedded clusters in galactic molecular clouds. In this article we review the current state of empirical knowledge concerning these extremely young protocluster systems. From a survey of the literature we compile the first extensive catalog of galactic embedded clusters. We use the catalog to construct the mass function and estimate the birthrate for embedded clusters within $\sim$2 kpc of the sun. We find that the embedded cluster birthrate exceeds that of visible open clusters by an order of magnitude or more indicating a high infant mortality rate for protocluster systems. Less than 4–7% of embedded clusters survive emergence from molecular clouds to become bound clusters of Pleiades age. The vast majority (90%) of stars that form in embedded clusters form in rich clusters of 100 or more members with masses in excess of 50 $M_{\odot}$. Moreover, observations of nearby cloud complexes indicate that embedded clusters account for a significant (70–90%) fraction of all stars formed in GMCs. We review the role of embedded clusters in investigating the nature of the initial mass function (IMF) that, in one nearby example, has been measured over the entire range of stellar and substellar mass, from OB stars to substellar objects near the deuterium burning limit. We also review the role embedded clusters play in the investigation of circumstellar disk evolution and the important constraints they provide for understanding the origin of planetary systems. Finally, we discuss current ideas concerning the origin and dynamical evolution of embedded clusters and the implications for the formation of bound open clusters.

1. INTRODUCTION

Stellar clusters have been long recognized as important laboratories for astrophysical research. Their study has played an important role in developing an understanding of the universe. For example, clusters contain statistically significant samples

of stars spanning a wide range of stellar mass within a relatively small volume of space. Because stars in such groups share the common heritage of being formed more or less simultaneously from the same progenitor molecular cloud, observations of cluster color-magnitude diagrams (CMDs) can be, and indeed, have been used to provide classical tests of stellar evolution theory. Moreover, clusters offer the smallest physical scale over which a meaningful determination of the stellar initial mass function (IMF) can be made. Because a cluster is held together by the mutual gravitational attraction of its individual members, its evolution is determined by Newton's laws of motion and gravity. In many body systems these interactions are inherently complex and thus clusters are also important testbeds for studies of stellar dynamics. The spatial distribution of clusters has also played a vital role in our understanding of galactic structure. The distribution of globular clusters, for example, was critical for determining the location of the galactic center, establishing the existence of a galactic halo and setting the overall scale of the Galaxy. Young open clusters have provided an important tracer of recent star formation in galaxies and of spiral structure in galactic disks. Such clusters are also of interest for understanding the origin of the solar system, because the presence of rare short-lived radio nuclides in meteoritic samples has long suggested that the sun was formed in near proximity to a massive star, and thus most likely within a relatively rich cluster.

Little is known or understood about the origin of clusters. Globular clusters in the Galaxy were formed billions of years ago. Because they are not being formed in the Milky Way in the present epoch of galactic history, direct empirical study of their formation process is not possible (except perhaps in certain extragalactic systems and at cosmological distances). On the other hand, open clusters appear to be continuously forming in the galactic disk and, in principle, direct study of the physical processes leading to their formation is possible. However, such studies have been seriously hampered by the fact that galactic clusters form in giant molecular clouds (GMCs) and during their formation and earliest stages of evolution are completely embedded in molecular gas and dust, and thus obscured from view. Given the constraints imposed by traditional techniques of optical astronomy, direct observation and study of young embedded clusters had been extremely difficult, if not impossible. However, during the past two decades the development of infrared astronomy and, more recently, infrared array detectors, has dramatically improved this situation. Figure 1 shows optical and infrared images of the southern embedded cluster RCW 38 and amply illustrates the power of infrared imaging for detecting such heavily obscured young clusters.

The deployment of infrared imaging cameras and spectrometers on optical and infrared optimized telescopes has provided astronomers the ability to survey and systematically study embedded clusters within molecular clouds. Almost immediately such studies indicated that rich embedded clusters were surprisingly numerous and that a significant fraction, if not the vast majority, of all stars may form in such systems. Consequently, it is now recognized that embedded clusters may be basic units of star formation and their study can directly address a number

of fundamental astrophysical problems. These include the issues of cluster formation and early evolution as well as the more general problems of the origin and early evolution of stars and planetary systems. Because most stars in the galactic disk may originate in embedded clusters, these systems must play a critical role in understanding the origins of some of the most fundamental properties of the galactic stellar population, such as the form and universality of the stellar IMF and the frequencies of stellar and planetary companions. The purpose of this review is to summarize the current status of observational knowledge concerning young embedded clusters in the Galaxy. We will consider both embedded and partially embedded clusters. The embedded phase of cluster evolution appears to last between 2 and 3 Myrs, and clusters with ages greater than 5 Myrs are rarely associated with molecular gas (Leisawitz, Bash & Thaddeus 1989) therefore, this review deals with clusters whose ages are typically between 0.5 and 3 Myrs. Particular emphasis will be placed on embedded clusters within $\sim$2 kpc of the sun because this presents a sample that is most statistically complete and for which the most detailed observational data are available. Previous reviews of embedded clusters, some with slightly different emphasis, can be found in various conference proceedings (e.g., Clarke, Bonnell & Hillenbrand 2000; Elmegreen et al. 2000; Lada 1998; Lada & Lada 1991; Lada et al. 2002; Zinnecker, McCaughrean & Wilking 1993).

2. EMBEDDED CLUSTERS: BASIC OBSERVATIONAL DATA

2.1. Definitions and Terminology

For the purposes of this review we consider clusters to be groups of stars that are physically related and whose observed stellar mass volume density would be sufficiently large, if in a state of virial equilibrium, to render the group stable against tidal disruption by the galaxy (i.e., $\rho_* \geq 0.1\ M_\odot\ \mathrm{pc}^{-3}$; Bok 1934), and by passing interstellar clouds (i.e., $\rho_* \geq 1.0\ M_\odot\ \mathrm{pc}^{-3}$; Spitzer 1958). Furthermore, we adopt the additional criterion (e.g., Adams & Myers 2001) that the cluster consists of enough members to insure that its evaporation time (i.e., the time it takes for internal stellar encounters to eject all its members) be greater than 10^8 years, the typical lifetime of open clusters in the field. The evaporation time, τ_{ev}, for a stellar system in virial equilibrium, is of order $\tau_{ev} \approx 10^2 \tau_{relax}$, where the relaxation time is roughly $\tau_{relax} \approx \frac{0.1N}{lnN}\tau_{cross}$, and τ_{cross} is the dynamical crossing time of the system while N is the number of stars it contains (Binney & Tremaine 1987). The typical crossing time in open clusters is of order 10^6 years, so if such a cluster is to survive disintegration by evaporation for 10^8 years, its relaxation time must be comparable to or greater than its crossing time or $\frac{0.1N}{lnN} \approx 1$. This condition is met when $N \approx 35$. Therefore, for this review, we define a stellar cluster as a group of 35 or more physically related stars whose stellar mass density exceeds $1.0\ M_\odot\ \mathrm{pc}^{-3}$.

With our definition we distinguish clusters from multiple star systems, such as small (N $<$ 6) hierarchical multiples and binaries, which are relatively stable systems and small multiple systems of the Trapezium type, that are inherently

unstable (Ambartsumian 1954, Allen & Poveda 1974). We also distinguish clusters from stellar associations, which we define as loose groups of physically related stars whose stellar space density is considerably below the tidal stability limit of 1 $M_{\odot}$ year^{-3} (Blaauw 1964). Clusters, as defined above, can be classified into two environmental classes depending on their association with interstellar matter. Exposed clusters are clusters with little or no interstellar matter within their boundaries. Almost all clusters found in standard open cluster catalogs (e.g., Lynga 1987) fall into this category. Embedded clusters are clusters that are fully or partially embedded in interstellar gas and dust. They are frequently completely invisible at optical wavelengths and best detected in the infrared. These clusters are the youngest known stellar systems and can also be considered protoclusters, because upon emergence from molecular clouds they will become exposed clusters. A similar classification can be applied to associations.

Our definition of a cluster includes stellar systems of two dynamical types or states. Bound clusters are systems whose total energy (kinetic + potential) is negative. When determining the total energy, we include contributions from any interstellar material contained within the boundaries of the cluster. We define a classical open cluster as a bound exposed cluster, such as the Pleiades, which is stable against tidal disruption for at least 10^8 years in the vicinity of the sun. Unbound clusters are systems whose total energy is positive. That is, unbound clusters are clusters of 35 or more stars whose space densities exceed 1 $M_{\odot}$ pc^{-3} but whose internal stellar motions are too large to be gravitationally confined by the stellar and nonstellar material within the boundaries of the cluster.

2.2. Identification and Surveys

Infrared surveys of molecular clouds are necessary to reveal embedded clusters because many, if not all, of their members will be heavily obscured. The initial identification of an embedded cluster is typically made by a survey at a single infrared wavelength (e.g., 2.2 μm or K band). The existence of a cluster is established by an excess density of stars over the background. In general the ease of identifying a cluster depends sensitively on the richness of the cluster, the apparent brightness of its members, its angular size or compactness, its location in the galactic plane and the amount of obscuration in its direction. For example, it would be particularly difficult to recognize a spatially extended, poor cluster of faint stars located in a direction where there is a high background of infrared sources, (e.g., $l = 0.0, b = 0.0$).

Identification of the individual members of a cluster is considerably more difficult than establishing its existence. In particular, for most clusters the source density of intrinsically faint members is usually only comparable to or even significantly less than that of background/foreground field objects. In such circumstances cluster membership can be determined only on a statistical basis, by comparison with star counts in nearby control fields off the cluster. However, determining whether or not a specific star in the region is a cluster member is not generally possible

from a star counting survey alone. In situations where field-star contamination is nonnegligible, other independent information (e.g., proper motions, spectra, multiwavelength photometry) is required to determine membership of individual stars.

The first deeply embedded cluster identified in a molecular cloud was uncovered in near-infrared surveys of the Ophiuchi dark cloud first made nearly thirty years ago using single-channel infrared photometers (Grasdalen, Strom & Strom 1974; Wilking & Lada 1983). However, not until the deployment of infrared imaging cameras in the late 1980s were large numbers of embedded clusters identified and studied. In a search of the astronomical literature since 1988, we have found that well over 100 such clusters have been observed both near the sun (e.g., Eiroa & Casali 1992) and at the distant reaches of the galaxy (e.g., Santos et al. 2000). To date, embedded clusters have been discovered using three basic observational approaches: 1. case studies of individual star forming regions, such as, for example, NGC 2282 (Horner, Lada & Lada 1997), LKHα 101 (Barsony, Schombert & Kis-Halas 1991), and NGC 281 (Megeath & Wilson 1997); 2. systematic surveys of various signposts of star formation, such as outflows (Hodapp 1994), luminous IRAS sources (e.g., Carpenter et al. 1993), and Herbig AeBe stars (Testi, Natta & Palla 1998); and 3. systematic surveys of individual molecular cloud complexes (e.g., Carpenter 2000; Carpenter, Heyer & Snell 2000; Carpenter, Snell & Schloerb 1995, 2000; EA Lada et al. 1991a; Phelps & Lada 1997). To date, most known embedded clusters have been found in surveys of star-formation signposts (see the second observational approach listed above), in particular the Hodapp (1994) survey of outflows has had by far the most prolific success rate. In the near future, we expect surveys conducted using the data generated by the all sky near-infrared surveys [i.e., Deep Near Infrared Survey (DENIS) and 2-Micron All-Sky Survey (2MASS)] will likely provide the the most systematic and complete inventory of the embedded cluster population of the Galaxy (e.g., Dutra & Bica 2001).

2.3. The Embedded Cluster Catalog

We have compiled a catalog of embedded clusters within $\sim$2 kpc of the sun. The catalog is based on a search of the astronomical literature since 1988. This search produced information on well over 100 clusters, most of which were identified in various systematic surveys (e.g, EA Lada et al. 1991b, Hodapp 1994, Carpenter Heyer & Snell 2000). From this list, we selected 76 clusters that met the following criteria: 1. evidence for embedded nature by association with a molecular cloud, HII region, or some significant degree of optical obscuration or infrared extinction; 2. identification of 35 or more members above field-star background within the cluster field; and 3. location within $\sim$2 kpc of the sun. Because of the large distance uncertainties of regions slightly beyond 2.0 kpc, such as the W3 molecular clouds (1.8–2.4 kpc), we have included clusters with published distance estimates of up to 2.4 kpc. Our catalog of nearby embedded clusters is presented in Table 1, which lists the cluster name, approximate location, distance, radius, number of members, and absolute magnitude limits of the corresponding imaging observations. These data were compiled from the references listed in the last column.

TABLE 1 Catalog of embedded clusters

EC	Name	RA (J2000)	Dec (J2000)	Distance (pc)	Size (pc)	N_*	K (limit)	Mass $M_\odot$	References
1	NGC 281W	00:52:23.7	+56:33:45	2100		231	18.0	130	1, 2
2	NGC 281E	00:54:14.7	+56:33:22	2100		88	17.0	57	1
3	01546 + 6319	01:58:19.8	+63:33:59	2400	0.54	54	17.5	35	3
4	02044 + 6031	02:08:04.7	+60:46:02	2400	0.73	147	17.5	94	3
5	02048 + 5957	02:08:27.0	+60:11:46	2400	0.56	58	17.5	37	3
6	02054 + 6011	02:09:01.3	+60:25:16	2400	0.59	70	17.5	45	3
7	02175 + 5845	02:21:07.7	+58:59:06	2400	0.73	109	17.5	70	3
8	IC 1805W	02:25:14.5	+61:27:00	2300		79	17.0	57	1
9	W3IRS5	02:25:40.6	+62:05:52	2400		87	17.0	64	4
10	02232 + 6138	02:27:04.1	+61:52:22	2400	0.91	205	17.5	130	3
11	02245 + 6115	02:28:21.5	+61:28:29	2400	0.64	121	17.5	77	3
12	02407 + 6047	02:44:37.8	+60:59:53	2400	0.46	50	17.5	32	3
13	02461 + 6147	02:50:09.2	+61:59:58	2400	0.72	115	17.5	73	3
14	02484 + 6022	02:52:18.7	+60:34:59	2400	0.62	86	17.5	55	3
15	02497 + 6217	02:53:43.2	+62:29:23	2400	0.38	36	17.5	23	3
16	02541 + 6208	02:58:13.2	+62:20:29	2400	0.45	40	17.5	26	3
17	02570 + 6028	03:01:00.7	+60:40:20	2400	0.62	78	17.5	50	3
18	02575 + 6017	03:01:29.2	+60:29:12	2400	1	240	17.5	150	3
19	AFGL 4029	03:01:32.3	+60:29:12	2200		173	16.5	140	1
20	02593 + 6016	03:03:17.9	+60:27:52	2400	0.62	88	17.5	56	3

21	AFGL 437	03:07:25.6	+58:30:52	2000		122	17.0	79	1
22	AFGL 490	03:27:38.7	+58:46:58	900		45	16.5	25	1
23	NGC 1333	03:32:08.1	+31:31:03	318	0.49	143	14.5	79	5
24	IC 348	03:44:21.5	+32:10:16	320	1.0	300	15.0	160	6, 7
25	LKHalpha 101	04:30:14.4	+35:16:25	800		150	15.0	98	8, 9
26	AFGL 5142	05:30:45.6	+33:47:51	1800		60	16.0	50	1,2
27	OMC 2	05:35:27.3	−05:09:39	500		119	17.5	63	1
28	L1641 N	05:36:23.1	−06:23:40	500	0.33	43	14.7	24	1, 10
29	ONC/Trapezium	05:37:47.4	−05:21:46	450	3.8	1740	14.0	1100	11, 12
	Trapezium	05:37:47.4	−05:21:46	450	0.24	780	17.5	413	13
30	AFGL 5157	05:37:47.8	+31:59:24	1800		71	16.5	50	1
31	L1641C	05:38:46.9	−07:01:40	500	0.33	47	14.7	27	1, 10
32	S235B	05:40:52.5	+35:41:25	1800		300	16.5	220	1,2
33	NGC 2024	05:41:42.6	−00:53:46	400	0.88	309	14.0	180	14
34	NGC 2068	05:46:41.8	+00:06:21	400	0.86	192	14.0	110	14
35	NGC 2071	05:47:10.0	+00:19:19	400	0.59	105	14.0	60	14
36	S242	05:52:12.9	+26:59:33	2100		96	16.5	81	1
37	L1641S	05:52:28.9	−08:07:30	500	0.65	134	14.7	78	1, 10
38	MonR2	06:07:46.6	−06:22:59	800	1.85	371	14.0	340	11, 17
39	AFGL 6366S	06:08:40.9	+21:31:00	1500		550	18.0	300	1
40	Gem4	06:08:41.0	+21:30:49	1500	1.74	114	14.5	190	18
41	AFGL 5180	06:08:54.1	+21:38:24	1500		94	16.5	60	1
42	Gem1	06:09:05.4	+21:50:20	1500	1.22	56	14.5	95	18

(*Continued*)

TABLE 1 (*Continued*)

EC	Name	RA (J2000)	Dec (J2000)	Distance (pc)	Size (pc)	N_*	K (limit)	Mass $M_\odot$	References
43	IRAS 06068 + 2030	06:09:51.7	+20:30:04	1500	0.39	59	15.3	54	2
44	GGD 12–15	06:10:50.9	−06:11:54	800	1.13	134	16.5	73	1, 11
45	IRAS 06155 + 2319	06:18:35.1	+23:18:11	1600	0.43	38	15.3	41	2
46	MWC 137	06:18:45.5	+15:16:52	1300	0.4	59	16.5	35	15
47	RNO 73	06:33:31.0	+04:00:06	1600		43	16.5	28	1
48	NGC 2244	06:34:55.3	+04:25:13	1600		150+			19
49	NGC 2264	06:41:03.2	+09:53:07	800		360	14.0	330	1, 20
50	NGC 2282	06:46:51.0	+01:18:54	1700	1.6	111	15.0	170	16
51	S287 N	06:47:50.4	−02:12:54	1400		46	16.5	29	1
52	BSF 56	06:59:14.4	−03:54:51	1400		64	16.5	40	1
53	S 287 C	06:59:36.6	−04:40:22	1400		50	16.5	31	1
54	L 1654	06:59:41.7	−07:46:29	1100		415	17.0	230	1
55	BIP 14	08:15:14.8	−04:04:41	1400		98	16.5	61	1
56	RCW38	08:59:05.4	−47:30:42	1700		1300	18.0	730	21
57	NGC 3576	11:11:57.0	−61:18:54	2400		51	13.0	720	22
58	Rho Oph	16:27:01.6	−24:36:41	125		100	14.0	53	23
58	NGC 6334I	17:20:53.0	−35:46:57	1700	0.6	93	16.0	78	24
60	Trifid/M20	18:02:23.0	−23:01:48	1600		85	14.3	190	25
61	NGC 6530/M8	18:07:51.9	−24:19:32	1800		100+			28
62	M16/NGC6611	18:18:48.0	−13:47:00	1800		300	14.0	960	26

63	M17	18:20:26.0	−16:10:36	1800		100	12.8	890	27
64	MWC 297	18:27:39.5	−03:49:52	450	0.5	37	16.7	20	15
65	Serpens SVS2	18:29:56.8	+01:14:46	250		51	15.5	27	1, 29
66	S87E	19:46:19.9	+24:35:24	2110		101	15.2	180	30
67	R CrA	19:01:53.9	−36:57:09	130		40	16.5	22	1, 31
68	S88B	19:46:47.0	+25:12:43	2000		98	15.5	120	1
69	S 106	20:27:25.0	+37:21:40	600	0.3	160	14.0	120	32
70	W 75 N	20:38:37.4	+42:37:56	2000		130	16.5	99	1
71	L1228	20:57:13.0	+77:35:46	150		47	18.0	25	1
72	IC 5146	21:02:36.3	+47:27:59	1200		100			33
73	L988 e	21:03:57.5	+50:14:38	700		46	14.5	32	1
74	LKHalpha234	21:43:02.2	+66:06:29	1000		139	17.0	76	1
75	Cep A	22:56:19.0	+62:01:57	700		580	17.0	310	1
76	Cep C	23:05:48.8	+62:30:02	750		110	16.5	60	1

References: 1) Hodapp 1994; 2) Carpenter et al. 1993; 3) Carpenter et al. 2000; 4) Megeath et al. 1996; 5) Lada et al. 1996; 6) Muench et al. 2003; 7) Lada & Lada 1995; 8) Aspin & Barsony 1994; 9) Barsony et al. 1991; 10) Strom et al. 1993; 11) Carpenter 2000; 12) Hillenbrand & Carpenter 2000; 13) Muench et al. 2002; 14) E.A. Lada et al. 1991b; 15) Testi et al. 1998; 16) Horner et al. 1997; 17) Carpenter et al. 1997; 18) Carpenter et al. 1995; 19) Marshal et al. 1992; 20) Lada et al. 1993; 21) J.F. Alves, private communication; 22) Persi et al. 1994; 23) Kenyon et al. 1998; 24) Tapia et al. 1996; 25) Rho et al. 2001; 26) Chini et al. 1992; 27) C.J. Lada et al. 1991; 28) van den Ancker et al. 1997; 29) Eiroa & Casali 1992; 30) Chen et al. 2002; 31) Wilking et al 1997; 32) Hodapp & Rayner 1991; 33) Herbig & Dahm 2002.

Given the heterogeneous nature of the observations from which this sample is drawn, this catalog cannot be considered complete. In particular, Southern Hemisphere regions, such as the Vela complex are not well represented because little observational data exist for this portion of the Galaxy. In addition, at least 12 additional clusters have been identified in the Rosette GMC (Phelps & Lada 1997), North American and Pelican nebulae (Cambresy, Beichman & Cutri 2002), and Cygnus X region, but no properties have been presented in the literature for them, and they are not included in our cluster catalog. Also there is a general incompleteness for the more distant clusters owing to sensitivity limitations. We estimate below that this 2-kpc sample is complete to only factors of 3–4. Although not complete, the catalog is, however, likely representative of the basic statistical properties of embedded clusters within $\sim$2 kpc. This is because a significant portion of the catalog comprises clusters drawn from systematic imaging surveys of individual cloud complexes and a survey (Hodapp 1994) that is reasonably complete for clusters associated with outflows, a primary tracer of very recent star-formation activity in molecular clouds. Moreover, the subset of clusters found in systematic surveys of nearby GMCs (Orion, Monoceros, and Perseus) is also likely to be reasonably complete for clusters with 35 or more members.

2.4. The Embedded Cluster Mass Function

Masses were derived for each cluster in the catalog by assuming a universal IMF for all the clusters. We adopted the IMF of the Trapezium cluster that was derived by Muench et al. (2002) from modeling of the cluster's K-band luminosity function (KLF). We then used the KLF models of Muench et al. (2002) to predict infrared source counts as a function of differing limiting magnitudes for two model clusters whose ages correspond to that of the Trapezium (0.8 Myrs) and IC 348 (2 Myrs) clusters. This was necessary to attempt to account for the expected luminosity evolution of the pre–main sequence (PMS) populations of embedded clusters (see discussion below in Section 4). A conversion factor from total source counts (for a given limiting magnitude) to total mass was then determined for each synthetic cluster. The infrared source counts listed for each observed cluster in the catalog were adjusted for distance and variable detection limits and then directly compared with the two model predictions. In most cases the near-infrared limits are faint enough (i.e., the IMF is reasonably sampled) that both models yielded cluster masses that agree extremely well for the two different ages. Given that no age information is available for the bulk of the clusters in the catalog, we adopted a conversion factor that was the average of the Trapezium and the IC 348 cluster ages. Additionally, we assumed that all clusters have an average extinction of 0.5 mag in the K band. The masses we have derived are probably uncertain by less than a factor of 2 for most clusters. The derived cluster masses in our sample range from about 20 to 1100 $M_{\odot}$. In Figure 2 (left panel) we present the embedded cluster mass distribution function (ECMDF) for all the clusters in our sample. The ECMDF was derived by summing individual embedded cluster masses (M_{ec}) in

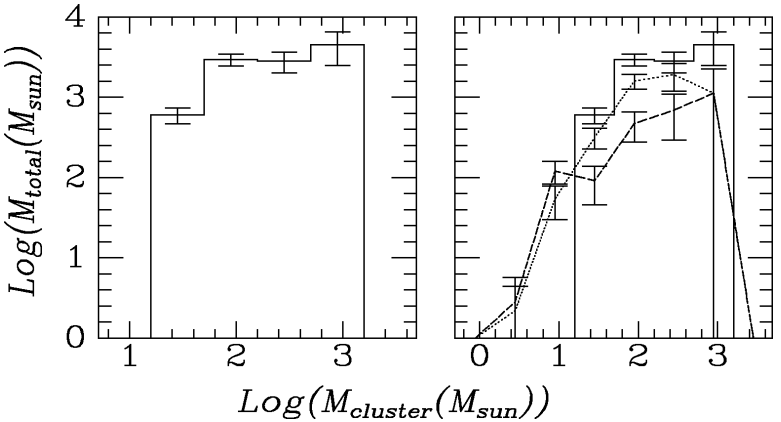

Figure 2 The embedded cluster mass distribution function (ECMDF) for the entire embedded cluster catalog is displayed in the left panel. This plot traces the distribution of total cluster mass (i.e., $N \times M_{EC}$) as a function of log mass (log(M_{EC})). The ECMDF is flat for clusters with masses between ∼50 and 1000 $M_\odot$. This corresponds to an embedded cluster mass function with a spectral index of −2 (i.e., $dN/dM \propto M^{-2}$). The right panel compares the ECMDF for the entire catalog with those of two cluster subsamples that are believed to be more complete at the lowest masses. The dotted line is the Hodapp outflow sample, and the dashed line is the sample of all known embedded clusters within 500 pc of the sun. The ECMDFs all appear to decline below 50 $M_\odot$.

evenly spaced logarithmic mass bins, 0.5 dex in width, beginning at Log (M_{ec}) = 1.2. (The boundaries of the bins were selected to insure that the least populated bin would have more than one object.) The ECMDF is equal to $M_{ec} \times$ dN/dlog M_{ec}, and thus differs by a factor of M_{ec} from the mass function (dN/dlog M_{ec}) of embedded clusters.

The histogram with the solid line represents the ECMDF for the entire cluster catalog (i.e., for clusters having $N_* > 35$ and $D < 2.4$ kpc). The mass distribution function displays two potentially significant features. First, the function is relatively flat over a range spanning at least an order of magnitude in cluster mass (i.e., $50 \leq M_{ec} \leq 1000\ M_\odot$). This indicates that, even though rare, 1000 $M_\odot$ clusters contribute a significant fraction of the total stellar mass, the same as for the more numerous 50–100 $M_\odot$ clusters. Moreover, more than 90% of the stars in clusters are found in clusters with masses in excess of 50 $M_\odot$ corresponding to populations in excess of 100 members. The flat mass distribution corresponds to an embedded cluster mass spectrum (dN/dM_{ec}) with a spectral index of −2 over the same range. This value is quite similar to the spectral index (−1.7) typically derived for the mass spectrum of dense molecular cloud cores (e.g., Lada, Bally & Stark 1991c). The fact that the embedded cluster mass spectrum closely resembles that of dense cloud cores is very interesting and perhaps suggests that a uniform star-formation

efficiency (SFE) characterizes most cluster-forming dense cores. The index for the mass spectrum of embedded clusters is also essentially the same as that (-1.5 to -2) of classical open clusters (e.g., Elmegreen & Efremov 1997, van den Bergh & Lafontaine 1984).

The second important feature in the ECMDF is the apparent drop off in the lowest-mass bin ($\sim$20–50 $M_{\odot}$). Given that our cluster catalog only included clusters with more than 35 stars, it is likely that we will be considerably more incomplete for clusters in the range of 20 to 50 $M_{\odot}$ than for the higher-mass clusters. To test the significance of this fall off to low cluster masses, we consider the mass distribution function of a subset of clusters drawn from a sample of local clouds where observations are reasonably complete. These were selected from systematic large-scale NIR surveys of four molecular clouds (L1630, L1641, Perseus, and Mon R2) without applying any lower limit to the size of the cluster population. Therefore, this sample should be sensitive to the full-mass range of clusters in these representative GMCs. This local molecular cloud sample is plotted as a dashed line in the right panel of Figure 2. Although the statistical errors due to the small sample size are large, the local sample confirms that there is indeed a drop off in total cluster mass for the lowest-mass clusters. As a further check, we also plotted the ECMDF for the Hodapp (1994) sample, again without applying any lower limit to the richness of the cluster. We chose the Hodapp sample because it was selected from a complete sample of outflows, indicative of very young stellar objects and should not be biased to any particular mass range of clusters. All three samples are consistent with a fall off in the cluster mass spectrum below approximately 50 $M_{\odot}$. Even if the cluster samples are not formally complete, they should be representative of the total local cluster population within 2 kpc. Therefore, we concluded that the drop off in the ECMDF at masses less than 50 $M_{\odot}$ is significant. Consequently, there appears to be a characteristic cluster mass (50 $M_{\odot}$) above which the bulk of the star-forming activity in clusters is occurring. Recently, Adams & Myers (2001) suggested, based on dynamical modeling of open clusters and knowledge of the cluster formation rate, that most clustered star formation occurs in clusters with between 10 and 100 stars. However, our results imply that no more than approximately 10% of all stars are formed in such small clusters. The discrepancy results from the use by Adams & Myers (2001) of the Battinelli & Capuzzo-Dolcetta (1991) catalog of open clusters, which undercounts clusters with ages less than 3 Myrs and underestimates the cluster formation rate as discussed below.

Using the masses in Table 1, we can estimate the contribution to the star-formation rate made by embedded clusters. Because of the incompleteness of our sample, this estimate necessarily will be a lower limit. To minimize the effect of incompleteness, we can calculate the star-formation rate for the local ($d < 500$ pc) subset of clusters for which we are likely to be reasonably complete. For this subsample, we calculate a local star-formation rate of ≥ 1–3×10^{-9} $M_{\odot}$ year^{-1} pc^{-2} assuming typical embedded cluster ages of $\sim$1–2 Myrs. This rate is in reasonable agreement with the local star-formation rate of between 3 and

7×10^{-9} $M_\odot$ year^{-1} pc^{-2} derived from field stars by Miller & Scalo (1979). This suggests that embedded clusters may account for a large fraction of all star formation occurring locally as has been suggested by other considerations (E.A. Lada et al. 1991b, Carpenter 2000). Extending our sample to 1 and 2 kpc gives star-formation rates of 1–0.7×10^{-9} $M_\odot$ year^{-1} pc^{-2}, respectively (for $\tau_{age} \sim$ 1 Myrs). The systematic drop in the star-formation rate with distance likely reflects progressively more incomplete cluster surveys as we move to greater distances. If we assume that we are nearly complete for the local 0.5-kpc sample, then the drop in the calculated birthrates would imply that we are incomplete by factors of at least 3 to 4 for the 1- to 2-kpc samples.

2.5. Birthrates and Star Formation

The embedded cluster catalog can be used to estimate a lower limit to the birthrate of embedded clusters in molecular clouds. Early estimates of the embedded cluster birthrate, based primarily on the number of clusters in the Orion cloud complex, found the rate to be extremely high compared to the birthrate of classical open clusters, suggesting that only a small fraction of embedded clusters survived emergence from molecular clouds to become classical open clusters (Lada & Lada 1991). Our more extensive embedded cluster catalog with an order of magnitude more clusters allows for a straightforward but much more meaningful estimate of this important formation rate. For 53 clusters within 2.0 kpc, we estimate the formation rate to be between 2 and 4 Myrs^{-1} kpc^{-2} for assumed average embedded cluster ages of 2 and 1 Myrs, respectively. Although this rate is a lower limit, it is a factor of 8–16 times that (0.25 Myrs^{-1} kpc^{-2}) estimated for classical open clusters by Elmegreen & Clemens (1985) and 5–9 times that (0.45 Myrs^{-1} kpc^{-2}) estimated by Battinelli & Capuzzo-Dolcetta (1991) for a more complete open cluster sample within 2 kpc of the sun. This difference in birthrates between embedded and open clusters represents an enormous discrepancy and is of fundamental significance for understanding cluster formation and evolution.

By combining our embedded cluster catalog with the open cluster catalog of Battinelli & Capuzzo-Dolcetta (1991), we can examine the age distribution of all clusters, open and embedded, within 2 kpc of the sun. The Battinelli & Cappuzzo-Dolcetta catalog contains about 100 classical open clusters and is thought to be complete out to a distance of 2 kpc from the sun for clusters with $M_V < -4.5$. In Figure 3, we plot the distribution of ages of all known clusters both embedded and open within 2 kpc. Embedded clusters populate the lowest age bin. We have included only those embedded clusters with masses greater than 150 $M_\odot$ to correspond to the magnitude-limited selection of Battinelli & Cappuzzo-Dolcetta. This represents roughly one third of our sample of clusters with published distances of 2 kpc or less. The average mass of these embedded clusters is 500 $M_\odot$, the same as that estimated for the open cluster sample by Battinelli & Cappuzzo-Dolcetta (1991). The number of clusters is roughly constant as a function of age for at least 100 Myrs. In Figure 3, we also compare the merged cluster age distribution

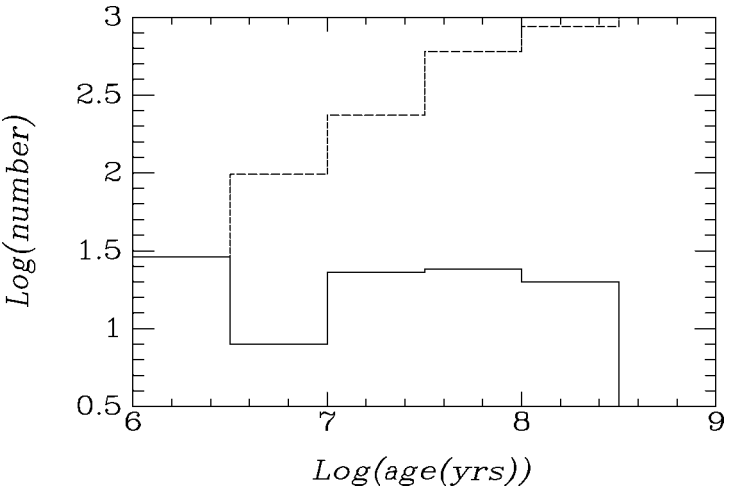

Figure 3 Observed frequency distribution of ages for open and embedded clusters within 2 kpc of the sun (*solid line*) compared to that predicted for a constant rate of star formation adjusted for cluster luminosity evolution (*dotted line*). All embedded clusters fall into the first bin. The large discrepancy between the predicted and observed numbers indicates a high infant mortality rate for protoclusters.

with the expected age distribution for a constant rate of cluster formation. Our prediction also includes an adjustment for the expected luminosity fading of clusters below the detection limits following the perscription of Battinelli & Cappuzzo-Dolcetta (1991). There is a large and increasing discrepancy between the expected and observed numbers. These distributions clearly confirm earlier speculations that the vast majority of embedded clusters do not survive emergence from molecular clouds as identifiable systems for periods even as long as 10 Myrs. Figure 3 suggests an extremely high infant mortality rate for clusters. Less than $\sim$4% of the clusters formed in molecular clouds are able to reach ages beyond 100 Myrs in the solar neighborhood, and less than 10% survive longer than 10 Myrs. Indeed, most clusters may dissolve well before they reach an age of 10 Myrs. If we consider our entire sample of embedded clusters, we predict, after similarly adjusing for fading, that at least 4100 clusters would be detected within 2 kpc of the sun with ages less than 300 Myrs. The WEBDA open cluster catalog (http://obswww.unige.ch/webda/) lists roughly 300 open clusters of this age or less within 2 kpc, suggesting that only approximately 7% of all embedded clusters survive to Pleiades age. It is likely that only the most massive clusters in our catalog are candidates for long-term survival. Roughly 7% of embedded clusters in our catalog have masses in excess of 500 $M_{\odot}$, and this likely represents a lower limit to the mass of an embedded cluster that can evolve to a Pleiades-like system. Clusters with ages in excess of 100 Myrs are very rare. This fact was first emphasized by Oort (1957) and then explained by Spitzer (1958), who demonstrated

that tidal encounters with passing interstellar clouds could disrupt all open clusters with mass densities $\leq 1\ M_{\odot}\ \mathrm{pc}^{-3}$ within 200 Myrs. In this context, it is interesting to note that both the infant mortality rate and life expectancy of clusters will be a function of distance from the galactic center. This is because both the galactic tidal force and the number of GMCs increase toward the center of the Galaxy, making encounters with GMCs both more frequent and disruptive. Indeed, van den Bergh & McClure (1980) pointed out that the oldest open clusters are strongly concentrated in the outer galaxy, a fact they attribute to a lower frequency of disruptive encounters with GMCs in the outer regions of the Galaxy. Moreover, Figure 3 also indicates that the disruption rate for bound clusters between 10 and 100 Myrs of age is significant, probably owing to encounters with GMCs. Many of the surviving open clusters observed in this age range may also not be presently stable (Battinelli & Capuzzo-Dolcetta 1991).

The discovery of large numbers of embedded clusters coupled with the high birthrates and star-formation rates we have inferred for them from our analysis of the data in Table 1 suggest that such clusters may account for a significant fraction of all star formation in the Galaxy. However, because of the incompleteness of our sample, it is difficult to produce an accurate estimate of the actual fraction of stars born in embedded clusters from statistical analysis of the data in our catalog. The best estimates of this quantity are derived from systematic, large-scale surveys of individual GMCs. The first systematic attempt to obtain an inventory of high- and low-mass YSOs in a single GMC was made by E.A. Lada et al. (1991b), who performed an extensive near-infrared imaging survey of the central regions (1 square degree) of the L1630 GMC in Orion. Their survey produced the unexpected result that the vast majority (60–90%) of the YSOs and star formation in that cloud occurred within a few (3) rich clusters with little activity in the vast molecular cloud regions outside these clusters. A subsequent survey by Carpenter (2000) using the 2MASS database to investigate the distribution of young stars in four nearby molecular clouds, including L1630, produced similar results with estimates of 50–100% of the clouds' embedded populations confined to embedded clusters. In both studies, the lower limits were derived with no correction for field-star contamination, which is substantial. Consequently, it is likely that the fraction of stars formed in clusters is very high (70–90%). Subsequent near-infrared surveys of L1630 (Li, Evans & Lada 1997) as well as other molecular clouds such as Mon OB1 (Lada, Young & Greene 1993), the Rosette (Phelps & Lada 1997), and Gem OB1 (Carpenter, Snell & Schloerb 1995) have yielded similar findings, suggesting that formation in clusters may be the dominant mode of formation for stars of all masses in GMCs and that embedded clusters may be the fundamental units of star formation in GMCs. Because GMCs account for almost all star formation in the Galaxy, most field stars in the Galactic disk may also have originated in embedded clusters. In this context, we note that it has long been recognized that most stars originate in OB associations (Roberts 1957), which in turn are formed from GMCs (Blitz 1980). The stellar component of an OB association, therefore, must consist primarily of the

remnants of dissolved embedded clusters. We discuss this point in more detail in Section 5.2.

2.6. Association with Molecular Gas and Dust

The intimate physical association with interstellar gas and dust is the defining characteristic of embedded clusters. Embedded clusters can either be partially (i.e., $A_V \sim 1$–5 mag.) or deeply (i.e., $A_V \sim 5$–100 mag) immersed in cold dense molecular material or hot dusty HII regions. The degree of their embeddedness in molecular gas is related to their evolutionary state. The least evolved and youngest embedded clusters (e.g., NGC 2024, NGC 1333, Ophiuchi, MonR2, and Serpens) are found in massive dense molecular cores, and the most evolved (e.g., the Trapezium, NGC 3603, IC 348) are located within HII regions and reflection nebulae or at the edge of molecular clouds. Our present understanding of the relation of dense cores and embedded clusters is largely guided by the coordinated surveys of such clouds as L1630 (Orion B), Gem OB1, and the Rosette (Mon OB2). These are the clouds for which the most systematic and complete surveys for both embedded clusters and dense molecular material exist (Lada 1992; Carpenter, Snell & Schloerb 1996; Phelps & Lada 1997). These studies all show that embedded clusters are physically associated with the most massive (100–1000 $M_\odot$) and dense ($n(H_2) \sim 10^{4-5}$ cm^{-3}) cores within the clouds. These cores have sizes (diameters) typically on the order of 0.5–1 pc. The typical SFEs (the instantaneous fraction of gas that has been processed into stars) range between 10% and 30% for these systems. The gas densities correspond to mass densities of 10^{3-4} $M_\odot$ pc^{-3}, suggesting that clusters with central densities of a few times 10^3 $M_\odot$ pc^{-3} can readily form from them.

Typically less than 10% of the area and mass of a GMC is in the form of dense gas. This gas is nonuniformly distributed through the cloud within numerous discrete and localized cores. These cores range in size between ~0.1 and 2 pc and in mass between a few solar masses and up to a thousand solar masses. The largest cores that spawn clusters are highly localized and occupy only a very small fraction (a few percent) of the area of a GMC. Numerous studies have indicated that the mass spectrum ($\frac{dN}{dm}$) of dense molecular cloud cores is a power-law with an index of $\alpha \sim -1.7$ (e.g., Lada, Bally & Stark 1991a; Blitz 1993; Kramer et al. 1998). For such a power-law index, most of the mass of a cloud's dense gas will be found in its most massive cores, even though low-mass cores outnumber high-mass cores. Stars form in dense gas; therefore, it is not surprising that a high fraction of all stars form in highly localized rich clusters because most of a cloud's dense gas is contained in its localized massive cores. Moreover, as discussed above, the mass spectrum of cores is very similar to that of both embedded and classical open clusters.

Not all massive dense cores in molecular clouds are presently forming clusters (e.g., Lada 1992). However, in the L1630 cloud, the cores with clusters appear to contain more gas at very high density ($n(H_2) > 10^5$ cm^{-3}) and to be more highly clumped or structured than those cores without clusters (Lada, Evans & Falgarone 1997). Whether this difference in physical properties is a cause or a

result of the formation of a cluster in a massive core is unclear. Studies of the distribution of dust continuum emission in the Ophiuchi (Motte, Andre & Neri 1998), Serpens (Testi & Sargent 1998), and the NGC 2068/2071 (Motte et al. 2001) cluster-forming cores reveal numerous small-scale ($\sim$5000 AU) clumps whose mass spectra are characterized by power-law slopes steeper than those of cloud cores but very similar to those that characterize the stellar IMF (see below). This would suggest that there is a direct mapping of clump mass to stellar mass and that the substructure of cluster-forming cores reflects the initial conditions of the star-formation process in dense cores. However, detailed observations of the NGC 1333 cluster-forming core paint a very different picture. Here, the density structure appears to be defined by numerous shells and cavities associated with intense outflow activity (Sandell & Knee 2001, Lefloch et al. 1998). This suggests that much of the structure in the core is the result of excavation by outflows from the young stars themselves and is a post- rather than pre-star-formation condition in this and perhaps other cores where outflow activity is occurring. In this regard it would certainly be interesting to obtain high-resolution dust continuum maps of the massive cores that are not forming clusters to see if the mass spectra of pre-stellar clumps in cores for which active star formation has not yet taken place are similar to those in cores in which star formation is already under way. A significant difference could implicate outflow activity as an agent that transforms an initial cloud-like clump mass spectrum into a clump spectrum more similar to that of stars.

2.7. Internal Structure and Mass Segregation

The structure of an embedded cluster is of great interest since it likely possesses the imprint of the physical process responsible for its creation. In particular, structure in the youngest embedded clusters reflects the underlying structure in the dense molecular gas from which they formed. Although all embedded clusters appear to display structure at some level, they can be characterized by two basic structural types: 1. Hierarchical-type clusters exhibit surface density distributions with multiple peaks and often significant structure over a large range of spatial scale. 2. Centrally condensed–type embedded clusters exhibit highly concentrated surface density distributions with relatively smooth radial profiles that can be described to a good approximation by simple power-law functions (e.g., $\rho_*(r) \sim r^{-q}$) or King-like (isothermal) potentials. In this sense, they are similar to classical open clusters. The relative frequency of these two types of structure in clusters is presently unknown, although there are clear examples of each in the literature.

Examples of hierarchical-type clusters include the deeply embedded double cluster NGC 1333 (Lada, Alves & Lada 1996) and the partially embedded cluster NGC 2264 that is highly structured (Lada, Green & Young 1992; Piche 1993). Figure 4 shows a map of the spatial distribution of infrared sources in the NGC 2264 cluster constructed from the data of Lada, Green & Young (1992). The cluster appears to be a double-double or quadruple cluster containing at least two levels of hierarchy in its spatial structure. The existence of hierarchical structure over large scales in star-forming regions has been well documented and is thought to

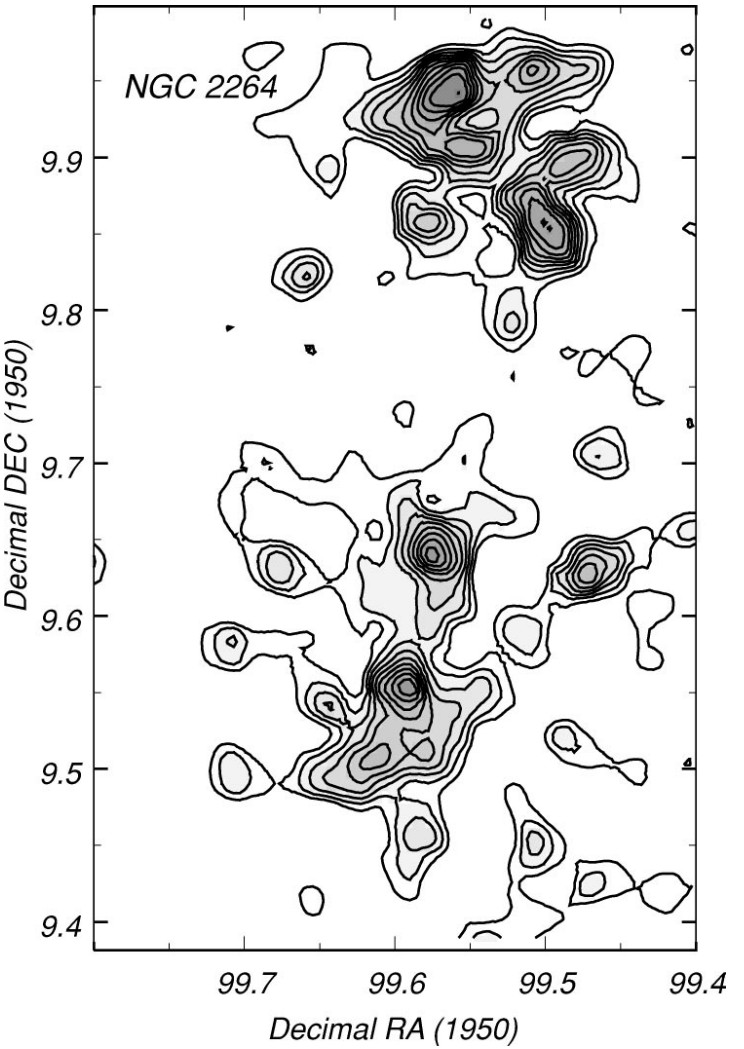

Figure 4 Contour map of the surface density of J-band infrared sources in the partially embedded cluster NGC 2264. This is an example of a cluster that displays a hierarchical structure.

be a signature of the turbulent nature of the interstellar gas and dust out of which GMCs, their dense cores, and ultimately stars form (e.g., Elmegreen et al. 2000).

The Trapezium-Orion Nebula Cluster (Trapezium-ONC cluster) (Hillenbrand & Hartmann 1998), IC 348 (Lada & Lada 1995, Muench et al. 2002), NGC 2024, NGC 2071 (E.A. Lada et al. 1991b), and NGC 2282 (Horner, Lada & Lada 1997) have strong central concentrations and radial surface density profiles that can

typically be fit by simple power-laws ($q \approx 1.5$) as well as King models. Such structure is a signature of the global dominance of gravity (over turbulence, for example) in the formation of these systems. Whether this structure is a primordial property of these clusters or a result of evolution from an initially more structured and hierarchical state is not clear. It is interesting to note in this context that each of these clusters is about the spatial extent of a single subcluster in NGC 2264. Overall, the centrally condensed clusters do exhibit some structure, but it is considerably less dramatic and more subtle than that observed in clusters such as NGC 2264. For example, Lada & Lada (1995) documented a handful of small, satellite subclusters in the outer regions of IC 348. However, given the small numbers of stars within them, one cannot rule out the hypothesis that these structures are merely the expected spatial fluctuations in the overall power-law falloff of the cluster's radial density distribution. Images of the Trapezium cluster in L band (3.4 μm) revealed that approximately 10% of the sources in the cluster belong to a deeply embedded population, whose surface density distribution differs from that of the main (less buried) cluster (Lada et al. 2000). In particular, the surface density distribution of the embedded population has a different orientation being more closely aligned with the ridge of molecular gas and dust at the back of the cluster. This population is also not nearly as centrally condensed. Another indication of subtle structure in the Trapezium-ONC and IC 348 clusters is the evidence for a spatial variation in the clusters' mass functions, both of which appear to exhibit an excess of the lowest-mass stars in their outer regions, perhaps suggestive of some degree of mass segregation (Hillenbrand & Carpenter 2001, Muench et al. 2002).

The question of mass segregation in embedded clusters is of great interest. Evidence for mass segregation in open clusters is well documented (e.g., Elmegreen et al. 2000) and likely caused by dynamical evolution and equipartition of energy in those systems. But is mass segregation also a primordial property of clusters or only achieved after significant dynamical evolution? Bonnell & Melvyn (1998) have argued that embedded clusters, like the Trapezium, are too young to have dynamically evolved significant mass segregation. If there is mass segregation in this cluster, it must be imprinted by the star-formation process. The strongest indication of possible mass segregation in embedded clusters derives from observations suggesting that the most massive stars in some of these systems are preferentially found near the cluster centers. This phenomenon has been observed in the Trapezium (Hillenbrand & Hartmann 1998), NGC 2071, and NGC 2024 (Lada et al. 1991b). Nurnberger & Petr-Gotzens (2002) found a steepening of the mass function in the outer region of NGC 3603, and Jiang et al. (2002) found an exponential, rather than power-law, radial decline of massive OB stars in M17, suggesting perhaps more extensive mass segregation in these more massive clusters. Similarly, *HST* observations of two rich clusters in the LMC indicate clear evidence for a steepening of the cluster luminosity functions, with increasing cluster radius indicating that mass segregation has taken place in these clusters (de Grijs et al. 2002). In other embedded clusters, such as MonR2, no evidence has

been found for any significant mass segregation (Carpenter et al. 1997). Indeed, there are even examples where the high-mass stars are found in the outer regions as well as the central regions of a cluster (e.g., IC 5146) (Herbig & Dahm 2002). The extent of the phenomenon of mass segregation in embedded clusters remains far from clear. Unfortunately, the inherent uncertainties due to small number statistics make it difficult to definitively investigate this issue in all but the most rich and massive clusters, which themselves are rare and typically very distant.

2.8. Ages and Age Spreads

The ages and age spreads of embedded clusters and their members are fundamental parameters that are among the most uncertain and difficult to determine for such young systems. Knowledge of these two timescales is critical for understanding the evolutionary appearance and state of a cluster and its star-formation history. For example, the ratio of cluster age, τ_{age}, to such timescales as the crossing time (τ_{cross}), the relaxation time, (τ_r), and the evaporation time (τ_{ev}) determines the dynamical state of the cluster. The relation between τ_{age} and the various timescales of early stellar evolution determines the evolutionary demographics of cluster members (e.g., the number of cluster members that are protostars, or PMS stars with and without disks). Indeed, as discussed below, the duration of the protostellar and disk phases of early stellar evolution can be inferred from knowledge of τ_{age} and an observational census of either the protostars or disk-bearing stars (respectively) within a cluster, or a sample of clusters of varying age. The age spread, $\Delta\tau_{sf}$, gives the duration of star formation or the gestation timescale for the cluster population. Also of interest is the star-formation rate, which is essentially given by the ratio of the number of cluster members to the gestation timescale (i.e., $N_*/\Delta\tau_{sf}$). These latter timescales provide important constraints for understanding the physical process of star formation within the cluster. Finally, embedded cluster ages are critical for dating molecular clouds, because cloud ages cannot be determined from observations of the dust and gas within them. The age of an embedded cluster provides an interesting lower limit to the age of the molecular cloud from which it formed. Indeed, the relative absence of molecular emission from around clusters with ages in excess of 5 Myrs, has long suggested that the lifetimes of molecular clouds typically do not exceed 5–10 Myrs (Leisawitz et al. 1989).

The most reliable method for age dating clusters and their members is through use of the Hertzberg-Russell diagram (HRD), where the positions of member stars are compared with the locations of theoretical PMS evolutionary tracks. Unfortunately, the theoretical trajectories of PMS stars on the HRD can be highly uncertain, particularly for cluster ages of 1 Myrs or less and for low-mass stars and substellar objects (e.g., Baraffe et al. 2002). In addition, empirical measurements of the two stellar parameters (i.e., luminosities and effective temperatures) that are necessary for placement of individual stars on the HRD can be very difficult owing to factors such as extinction, stellar variability, binarity, veiling, and infrared

excess, which are common characteristics of PMS stars. Moreover, often such measurements can only be carried out at infrared wavelengths. As a result of these various factors, the ages of embedded clusters are inherently uncertain and often very poorly constrained by observations.

In practice, it is often more straightforward to place stars on the CMD and then transform the theoretical tracks to that observational plane for comparison and cluster age determinations. There exist only a small number of embedded clusters, such as NGC 2024 (M.R. Meyer, unpublished PhD thesis), IC 348 (Herbig 1998), the Trapezium (Hillenbrand 1997), NGC 2264 (Park et al. 2000), and IC 5146 (Herbig & Dahm 2002), for which sufficient observations are available to place a significant sample of sources on the CMD and estimate their ages. Published estimates for the mean ages of these clusters vary between 0.5 and 3 Myrs. Unfortunately, the uncertainties introduced by using PMS tracks can be on the order of the derived age of the cluster. For example, Park et al. (2000) derived the age of NGC 2264 using four different PMS models with resulting values of 0.9, 2.1, 2.7, and 4.3 Myrs for the age of the cluster. Another problem is that an individual PMS model can give different ages for high- and low-mass stars in the same cluster (e.g., Hillenbrand 1997). On the other hand, the relative mean ages of young clusters can be established to much greater precision by using a single or consistent set of PMS models to extract the cluster ages (e.g., Haisch et al. 2001a).

Published comparisons of embedded cluster HRDs or CMDs with theoretical PMS tracks indicate age spreads that are usually of the same order or even greater than the mean cluster ages. For example, age spreads of 5.5, 8.0, 10.0, and 15.3 Myrs were found using four different PMS models for the 2–3-Myrs-old cluster NGC 2264 by Park et al. (2000). A good example of an embedded cluster CMD is shown in Figure 5, which displays the CMD constructed by Herbig (1998) for the IC 348 cluster. The positions of suspected cluster members form a well-defined, but relatively wide, PMS. Comparison with the isochrones derived from a single set of PMS tracks gives a cluster mean age of $\sim$2 Myrs and an age spread of $\sim$5 Myrs. In principle, the detailed distribution of stars within the PMS band in the plane of the CMD reflects the star-formation history of the embedded population. Indeed, from a detailed examination of the distribution of stars in the HRDs of a number of embedded clusters (including the Trapezium, IC 348, NGC 2264, and Rho Ophiuchi), Palla & Stahler (2000a,b) produced intriguing evidence for a strongly time-dependent star-formation rate in these regions. Using a consistent analysis and a single set of PMS tracks, they found that star formation appeared to be accelerating with time, with the star-formation rate reaching its peak in the last 1–2 Myrs in all clusters still associated with significant molecular gas.

However, it is difficult to evaluate the significance of age spreads and distributions estimated from CMDs of embedded clusters because differential extinction, source variability, infrared excess, binarity, and contamination by field stars can contribute significantly to the intrinsic scatter in the diagram (e.g., Hartmann 2001). The uncertainties due to factors such as variability, infrared excess, and extinction are expected to be greater for younger clusters. Figure 6 shows the CMD

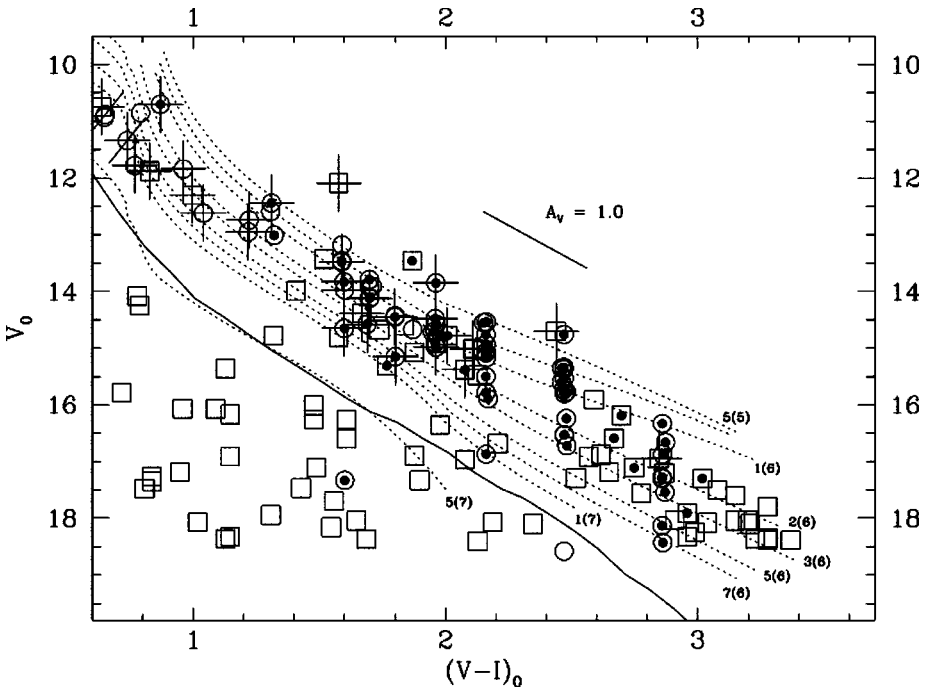

Figure 5 The V, V-I color-magnitude diagram (CMD) for IC 348 compiled by Herbig (1998). Circles are stars for which spectral types are known; solid dots indicate stars with Hα emission and, therefore, likely members. Theoretical isochrones derived from a single set of PMS tracks are shown and labeled by age [e.g., 3(6) corresponds to 3 Myrs]. The diagram shows that there is an appreciable spread in the locus of PMS stars in this cluster corresponding to an apparent age spread that is comparable to the mean age of the cluster.

obtained for NGC 2362, a 5-Myr-old, exposed, open cluster where such uncertainties should be minimized (Moitinho et al. 2001). The PMS of this cluster is very well defined and relatively narrow, indicating a clear upper limit to its age spread of less than 3 Myrs. In this cluster, where the total and differential extinction are barely measurable, and stellar activity associated with the youngest stars minimal, the CMD indicates a simple star-formation history characterized by cluster formation in a rapid, coeval burst of activity less than 3 Myrs in duration. These observations may also suggest that a significant portion of the observed scatter in the CMDs of other younger and embedded clusters is due to factors other than age. Unfortunately, it is presently not possible to determine whether the large spreads in embedded cluster CMDs result from a wide variety of gestation times, accelerating star formation or other factors. Because the number of embedded clusters with age determinations is small, a systematic and detailed examination of a larger sample of embedded and young open cluster CMDs would be useful in

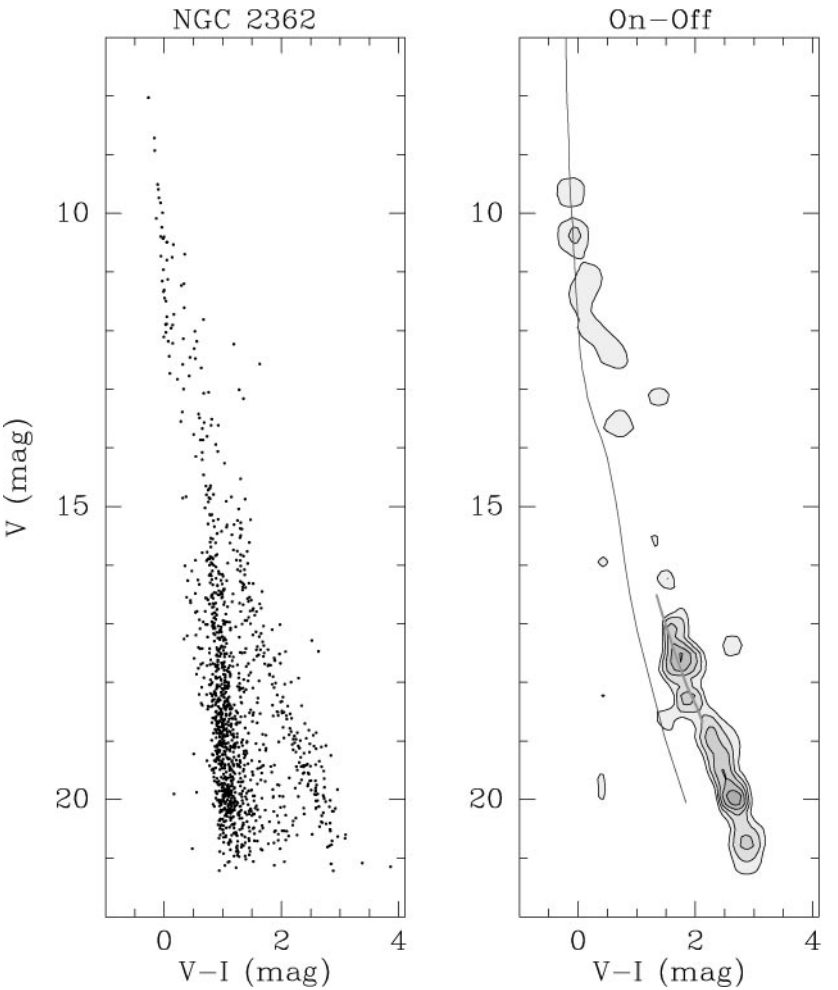

Figure 6 The V, V-I color-magnitude diagram (CMD) for the 5-Myr-old open cluster NGC 2362 (Moitinho et al. 2001). The left panel shows the CMD for all stars in the NGC 2362 field. A narrow, well-defined PMS band stretching over a range of at least 9 mag in V, from A stars to M stars, is evident. The right panel shows a contour plot of difference between the surface density of stars in the CMD of the cluster (on) and that of stars in the CMD of a nearby control field (off). The locus of points corresponding to the ZAMS and a 5-Myr-old PMS isochrone are also plotted for comparison. The narrow width of the cluster's PMS indicates that the cluster formed in a coeval burst of star formation less than 3 Myrs in duration. Figure courtesy of J. Alves.

resolving this issue. At present, self-consistent determinations of the mean ages and, in particular, the relative mean ages of clusters may be the most robust information about star-formation histories that can be extracted from CMD or HRD analysis.

3. EMBEDDED CLUSTERS AND THE IMF

3.1. Background

A fundamental consequence of the theory of stellar structure and evolution is that, once formed, the subsequent life history of a star is essentially predetermined by one parameter, its birth mass. Consequently, detailed knowledge of the initial distribution of stellar masses at birth (i.e., the IMF) and how this quantity varies through time and space is necessary to predict and understand the evolution of stellar systems, such as galaxies and clusters. Detailed knowledge of the IMF and its spatial and temporal variations is also particularly important for understanding the process of star formation because the mysterious physics of this process control the conversion of interstellar matter into stars. Unfortunately, stellar evolution theory is unable to predict the form of the IMF. This quantity must be derived from observations. However, this is not a straightforward exercise because stellar mass is not an observable quantity. Stellar radiant flux or luminosity is the most readily observed property of a star. Determination of stellar masses therefore requires a transformation of stellar luminosities into stellar masses, which in turn requires knowledge of stellar evolutionary states. Numerous techniques have been employed in an attempt to determine the IMF both for the galactic field-star population and in open clusters. These techniques and results have been extensively reviewed in the literature (e.g., Scalo 1978, 1986; Gilmore & Howell 1998; Meyer et al. 2000; Kroupa 2002). IMFs derived from these studies appear to exhibit two similar general properties. First, for stars more massive than the sun, the IMF has a nearly power-law form with the number of stars increasing as the stellar mass decreases. If we adopt the classical definition that the IMF ($\xi(\log m_*)$) is the number of stars formed per unit volume per unit logarithmic mass interval, then the slope at any point is $\beta \equiv \partial \log \xi(\log m_*)/\partial \log m_*$, and $\beta \approx -1.3$ for masses greater than one solar mass (e.g., Massey 1998). This is very similar to the value (–1.35) originally derived for field stars by Salpeter (1955). Second, the IMF breaks and flattens near but slightly below 1 $M_\odot$, departing significantly from a Salpeter slope. At the lowest masses (i.e., 0.5–0.1 $M_\odot$), however, there is considerable debate concerning whether the IMF declines, rises, or is flat and whether it extends smoothly below the hydrogen burning limit (HBL) to substellar masses.

However, IMF determinations for local field stars and in open clusters are hampered by a number of serious difficulties. To deduce the IMF for field stars requires compilation of a volume-limited sample of nearby stars. This, in turn, requires accurate distance measurements, usually parallaxes, for all stars in the sample. To obtain the necessary complete sample to as low a mass as possible

necessitates that this volume be limited to stars relatively near the sun (d $\sim$ 5–25 pc), because of the extreme faintness of the lowest-mass stars and the limitations inherent in the distance determinations. Such samples suffer from incompletness for both the highest-mass stars, because of their rarity and complete absence in the solar neighborhood, and the lowest-mass stars, because of their faintness. Moreover, such samples contain stars formed over a time interval encompassing billions of years (essentially the age of the galactic disk). Therefore, the mass function derived directly from observations of field stars is a present-day mass function (PDMF) and must be corrected for the loss of higher-mass stars caused by stellar evolution to derive the IMF of the sample. This, in turn, requires the assumptions of both a star-formation rate, usually taken to be constant, and a time independent functional form of the IMF. The standard final product is an IMF that is time-averaged over the age of the Milky Way disk. Details regarding any dependence of the IMF on either space or time over the history of the Galaxy are necessarily lost in the time-averaged IMFs derived from nearby field stars. Finally, it is very difficult to measure the IMF below the HBL from magnitude-limited studies of the field. This is because the luminosities of brown dwarfs continue to fade throughout their entire life history, so the number of substellar objects at any brightness is always a time-dependent mixture of brown dwarfs of varying mass and age, and it depends sensitively on the formation history of brown dwarfs in the Galactic disk.

Stellar clusters have played an important role in IMF studies because they present equidistant and coeval populations of stars of similar chemical composition. Compared with the disk population, clusters provide an instantaneous sampling of the IMF at different epochs in galactic history (corresponding to the different cluster ages) and in different, relatively small volumes of space. This enables investigation of possible spatial and temporal variations in the IMF. However, some of these advantages are mitigated by the larger distances of visible open clusters (compared to local field stars), which reduce the sensitivity to faint low-mass stars, and by field-star contamination that seriously hampers determination of cluster membership and achievement of completeness, especially at low masses. In addition, dynamical evolution produces both mass segregation and evaporation and depletes the low-mass population of clusters requiring uncertain corrections to be applied to obtain their IMFs. Also, stellar evolution depletes the high-mass end of the IMF in clusters older than 10 Myrs or so and thus must be accounted for as well.

Using young embedded clusters for IMF determinations alleviates many of these issues. For example, embedded clusters are often significantly more compact than visible open clusters minimizing field-star contamination, except at the very lowest masses. Moreover, the molecular gas and dust associated with such clusters can screen background stars even at faint magnitudes, further reducing background contamination and associated difficulties with membership determinations. In addition, embedded clusters are too young to have lost significant numbers of stars because of stellar evolution or dynamical evaporation, thus their

PDMFs are, to a very good approximation, their IMFs. Embedded clusters are also particularly well suited for determining the nature of the IMF for low-mass stars and substellar objects. This is because low-mass stars in embedded clusters are primarily PMS stars and thus are brighter than at any other time in their lives prior to their evolution off the main sequence. At these young ages, substellar objects or brown dwarfs are also significantly more luminous than at any other time in their subsequent evolution. Moreover, they have brightnesses comparable to the lowest-mass stars. Indeed, infrared observations of modest depth are capable of detecting objects spanning the entire range of stellar mass from 0.01 to 100 $M_{\odot}$ in clusters within 0.5–1.0 kpc of the sun.

However, the study of embedded clusters suffers from two disadvantages: 1. The clusters are often heavily obscured and cannot be easily observed at optical wavelengths; and 2. the stars in such clusters are mostly PMS stars, and the timescale for forming them is an appreciable fraction of the cluster age. Consequently, uncertain corrections for PMS evolution and noncoevality must be applied to the members to derive mass spectra from luminosity functions. Advances in infrared detectors have enabled the direct observation of such embedded clusters and helped minimize the first disadvantage. The second disadvantage requires modeling and is more difficult to overcome (e.g., Comeron et al. 1993, 1996; Fletcher & Stahler 1994a; Lada & Lada 1995; Lada, Lada & Muench 1998; Luhman et al. 2000; Meyer et al. 2000; Muench et al. 2000, 2002; Muench, Lada & Lada 2000; Zinnecker et al. 1993; and others). Finally, although the underlying mass functions of most embedded clusters are likely to be a fair representation of their IMFs, some embedded clusters can be expected to be in extremely early stages of evolution in which active star formation is still contributing to building the ultimate cluster IMF. Appropriate caution must be taken when interpreting the mass functions derived in such circumstances.

3.2. Methodology: From Luminosity to Mass Functions

Two basic methods have been generally employed to derive mass functions for embedded clusters. The first method involves modeling the observed luminosity function of an embedded cluster to derive the form of its underlying mass function (e.g., Fletcher & Stahler 1994a,b; Lada & Lada 1995; Megeath 1996; Muench et al. 2000, 2002; Zinnecker et al. 1993). The second method involves the use of spectroscopy and/or multicolor photometry to place individual stars on the HRD. Comparison of the locations of these stars in the HRD with the predictions of PMS evolutionary tracks results in the determination of their individual masses from which the cluster IMF is then directly constructed (e.g., Hillenbrand 1997, Hillenbrand & Carpenter 2000). As will be discussed below, these methods have their own advantages and disadvantages, but in general are complementary. Indeed, in a few studies, IMFs for embedded clusters have been derived using a combination of these and similar techniques (e.g., Comeron et al 1993, 1996; Luhman et al. 1998, 2000).

3.2.1. MODELING THE LUMINOSITY FUNCTION Deriving the IMF of an embedded cluster by modeling its luminosity function first requires the construction of the cluster's luminosity function. Although determining the bolometric luminosity function of a cluster would be most desirable for comparison with theoretical predictions (e.g., Fletcher & Stahler 1994a,b; Lada & Wilking 1984), obtaining the multiwavelength observations necessary to do so would require prohibitive amounts of observing time on telescopes both on the ground and in space. On the other hand, the monochromatic brightness of a star is its most basic observable property and infrared cameras enable the simultaneous measurement of the monochromatic brightnesses of hundreds of stars. Thus, complete luminosity functions, which span the entire range of stellar mass, can be readily constructed for embedded stellar clusters with small investments of telescope time. The monochromatic (e.g., K band) luminosity function of a cluster, $\frac{dN}{dm_K}$, is defined as the number of cluster stars per unit magnitude interval and is the product of the underlying mass function and the derivative of the appropriate mass-luminosity relation (MLR):

$$\frac{dN}{dm_K} = \frac{dN}{d\log M_*} \times \frac{d\log M_*}{dm_K}, \tag{1}$$

where m_k is the apparent stellar (K) magnitude, and M_* is the stellar mass. The first term on the right-hand side of the equation is the underlying stellar mass function, and the second term is the derivative of the MLR. With knowledge of the MLR (and bolometric corrections), this equation can be inverted to derive the underlying mass function from the observed luminosity function of a cluster whose distance is known. This method is essentially the one originally employed by Salpeter (1955) to derive the field-star IMF. However, unlike main-sequence field stars, PMS stars, which account for most of the stars in an embedded cluster, cannot be characterized by a unique MLR. Indeed, the MLR for PMS stars is a function of time. Moreover, for embedded clusters, the duration of star formation can be a significant fraction of the cluster's age. Consequently, to invert the equation and derive the mass function, one must model the luminosity function of the cluster, and this requires knowledge of the star-formation history (i.e., age and age spread) of the cluster as well as the time-varying PMS MLR. This presents the two major disadvantages for this technique. First, a priori knowledge of the age or star-formation history of the cluster is required, and this typically can be derived by placing cluster stars on an HRD. However, this in turn requires additional observations such as multiwavelength photometry or spectroscopy of a representative sample of the cluster members. Second, PMS models must be employed to determine the time-varying MLR. The accuracy of the derived IMF therefore directly depends on the accuracy of the adopted PMS models, which may be inherently uncertain, particularly for the youngest clusters ($\tau < 10^6$ years) and lowest-mass objects ($m < 0.08\ M_\odot$). In addition, most PMS models predict bolometric luminosities as a function of mass and time; thus, bolometric corrections must be used to transform the theoretical predictions to monochromatic fluxes and magnitudes.

Despite these complexities, Monte Carlo modeling of the infrared luminosity functions of young clusters (Muench, Lada & Lada 2000) has demonstrated that the functional form of an embedded cluster's luminosity function is considerably more sensitive to the form of the underlying cluster mass function than to any other significant parameter (i.e., stellar age distribution, PMS models, etc.). In fact, despite the significant differences between the parameters that characterize the various PMS calculations (e.g., adopted convection model, opacities, etc.), model luminosity functions are essentially insensitive to the choice of the PMS mass-to-luminosity relations. As discussed below, this reflects the robust nature of PMS luminosity evolution. There are, however, other limitations of this technique. In particular, the observed luminosity function of a cluster will always contain unrelated foreground and background field stars along with cluster members. Such field-star contamination can be straightforwardly corrected for by using imaging observations of nearby control fields. However, at the faintest magnitudes, often corresponding to the substellar mass regime, the field-star contamination can be severe and may introduce significant uncertainty in the faint end of the field-star-corrected luminosity function.

3.2.2. INDIVIDUAL STELLAR MASSES FROM THE HRD Deriving the IMF of an embedded population via the HRD requires simultaneous knowledge of both the luminosities and effective temperatures of all the stars in a cluster so that they can be individually placed on the HRD. This, in turn, requires both photometry to determine stellar luminosities and either colors or a spectrum of each star to determine effective temperature. For embedded clusters, spectroscopy is the preferred method of obtaining a stellar effective temperature because the infrared colors of stars are not intrinsically very sensitive to effective temperature and, in addition, are significantly altered by extinction and infrared excess associated with the young stars. The advantage of this method is that the final product is the set of individual masses for all stars for which both spectra and photometry were obtained. In other words, this procedure provides a more detailed determination of the mass function than the first method. In addition, this procedure also yields the ages of the stars and the star-formation history of the cluster. The major disadvantage of this method is that it requires spectra to be obtained for a complete sample of stars across the entire spectrum of stellar masses. As a result, a significant investment of integration and telescope time is required to obtain a complete sampling of the IMF, particularly at the faint, low-mass end. As with the first method, field-star contamination, particularly at the lowest masses, is a serious limitation. However, this limitation can be overcome with the acquisition of spectra for all stars (unrelated foreground and background stars plus members) within a cluster. But, at faint magnitudes, field stars can easily dominate cluster members, sharply decreasing observing efficiency. Thus sensitivity limitations inherent in spectroscopic observations ultimately restrict the application of this technique to a small number of nearby clusters.

Similar to the first method, the technique of deriving a PMS star's mass from its location on the HRD is also fundamentally limited by uncertain knowledge

of PMS evolutionary tracks. Indeed, the IMF derived by this technique is more sensitive to uncertainties in PMS models than the IMF derived by modeling stellar luminosities. This is because existing PMS models are able to predict the effective temperatures of PMS stars with considerably less certainty than their luminosities. This is illustrated in Figure 7, which compares the predictions of standard PMS models for luminosities and effective temperatures of PMS stars of the same age but varying mass. The predicted luminosities are essentially degenerate with respect to the PMS models used. Although perhaps surprising at first glance, this result can be understood by considering the fact that the luminosity of a PMS star is determined by very basic physics, simply the conversion of gravitational potential energy to radiant luminosity during Kelvin-Helmholtz contraction. This primarily depends on the general physical conditions in the stellar interior (e.g., whether the interior is radiative or partially or fully convective). The close agreement of the model predictions reflects the robust nature of PMS luminosity evolution. Predicting the effective temperature of such stars, which depends on detailed knowledge of uncertain characteristics (e.g., opacities) of the stellar atmospheres, is a more difficult exercise. These same models can predict very different locations for such stars on the HRD, corresponding to significant differences in the predicted masses and mass functions.

3.2.3. GENERAL LIMITATIONS Other limitations that hinder determinations of the IMFs of embedded clusters via any of the standard approaches include differential reddening of cluster members, presence of infrared excess, and veiling continuum emission. These effects need to be accounted for either in the modeling or by direct correction of the observed photometry and spectroscopy of individual sources using additional observations. Embedded clusters are also at sufficiently large distances that binary systems within them are almost always unresolved in typical observations. Consequently, the IMFs derived by these methods do not include the masses of any unresolved companions. Binary companions can affect the derivations of the IMFs in two ways. First, they can contribute additional flux to the system luminosity. However, because the vast majority of binaries are not equal mass (brightness) systems, this contribution is typically small (0.1–0.2 mag) (e.g., see Simon et al. 1995) compared to the typical bin sizes (0.5 mag) used to construct the infrared luminosity functions. Second, the presence of unresolved binaries can result in an underestimate of the numbers of low-mass stars in a cluster compared to that expected for a system of stars in which all binaries are resolved, because companion stars are not directly observed or counted (Kroupa et al. 1991). Thus, the IMFs that are derived are system- or primary-star IMFs. Whether such a primary-star IMF should be adjusted by adding in the masses of companion stars depends on the question being considered. For example, for comparisons with IMFs derived for field stars as well as open and globular clusters, the primary-star IMF is the appropriate IMF to use. If one desires to exactly weigh the amount of interstellar medium transformed into stars by the star-formation process, then a primary- + companion-star IMF would be the more appropriate

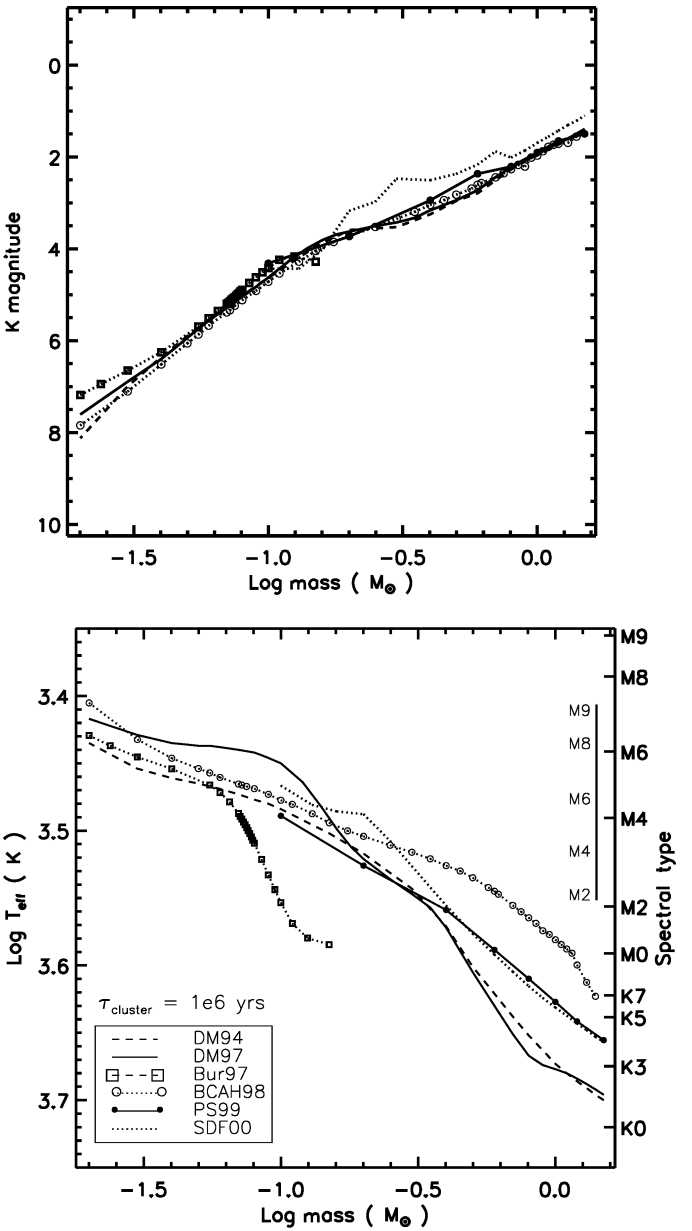

Figure 7 Comparison of theoretical predictions for the luminosities and effective temperatures of million-year-old PMS stars as a function of mass from a suite of standard PMS models (Burrows et al. 1997; Baraffe et al. 1998; D'Antona & Mazzitelli 1994, 1998; Palla & Stahler 1999; Seiss et al. 2000). The predicted K magnitudes of such stars (*top*) are in excellent agreement over the entire mass spectrum, whereas the predicted effective temperatures (*bottom*) are in relatively poor agreement.

mass function to consider. Unfortunately, the IMF of companion stars is not very well known or constrained by existing observational data, and determination of a total IMF including primary and companion stars is not presently possible. Finally, because the IMF is a statistical property of an ensemble of stars, it can only be meaningfully derived over a mass interval, which is statistically well sampled by observations. The richness of the observed cluster thus sets a basic limit on the level of uncertainty in any derived IMF.

3.3. The IMF of the Trapezium Cluster from OB Stars to Brown Dwarfs

The Trapezium cluster in Orion is the best studied of all embedded clusters. First identified by Trumpler (1931), and Baade & Minkowski (1937), the Trapezium cluster is a rich cluster of faint (mostly PMS) stars embedded within the Great Orion Nebula with an age of approximately 10^6 years (Hillenbrand 1997, Prosser et al. 1994). The cluster is approximately 0.3–0.4 pc in diameter (e.g., Lada et al. 2000) and contains approximately 700 stars (Hillenbrand & Carpenter 2000, Muench et al 2002). It is thought to be the highly concentrated core of the more extended ONC, which contains nearly 2000 stars spread over a region roughly 4 pc in extent (e.g., Hillenbrand & Hartmann 1998). At its center is the famous Trapezium, a close grouping of four OB stars that excite the nebula. It is a superb target for IMF studies because of its youth, richness, compactness, location in front of and partially within an opaque molecular cloud, and its proximity to the sun ($\sim$450 pc). These factors combine to enable a statistically significant sampling of the IMF from OB stars to substellar objects near the deuterium burning limit (0.01 $M_\odot$) with minimal field-star contamination. Indeed, this cluster is particularly well suited for investigating the substellar portion of the IMF and determining the initial distribution of masses for freely floating brown dwarfs. Deep infrared surveys of this cluster have been performed using the *HST* (Luhman et al 2000), the Keck Telescope (Hillenbrand & Carpenter 2000), UKIRT (Lucas & Roche 2000), and the NTT (Muench et al. 2002) and have produced infrared luminosity functions and mass functions that sample well into the substellar mass range.

Figure 8 shows a three-color infrared image of the cluster resulting from the NTT survey. Muench et al. (2002) used these data along with observations of the same region obtained with a 1.2-m telescope to recover the brighter stars typically saturated in deep exposures with the larger telescopes, and they produced a complete sampling of the K-band (2.2 μm) luminosity function (KLF) of this cluster spanning the mass range from OB stars to substellar objects near the deuterium burning limit. Figure 9 shows the field-star corrected, complete, extinction-limited KLF derived from the Muench et al. (2002) study. It counts all stars within a cloud depth of 17 mag of visual extinction with luminosities corresponding to million-year-old objects with masses $\sim$0.010–0.015 $M_\odot$ and greater and is representative of the infrared luminosity functions obtained in all similarly sensitive investigations of this cluster. In particular, the KLF rises steadily from the brightest stars to

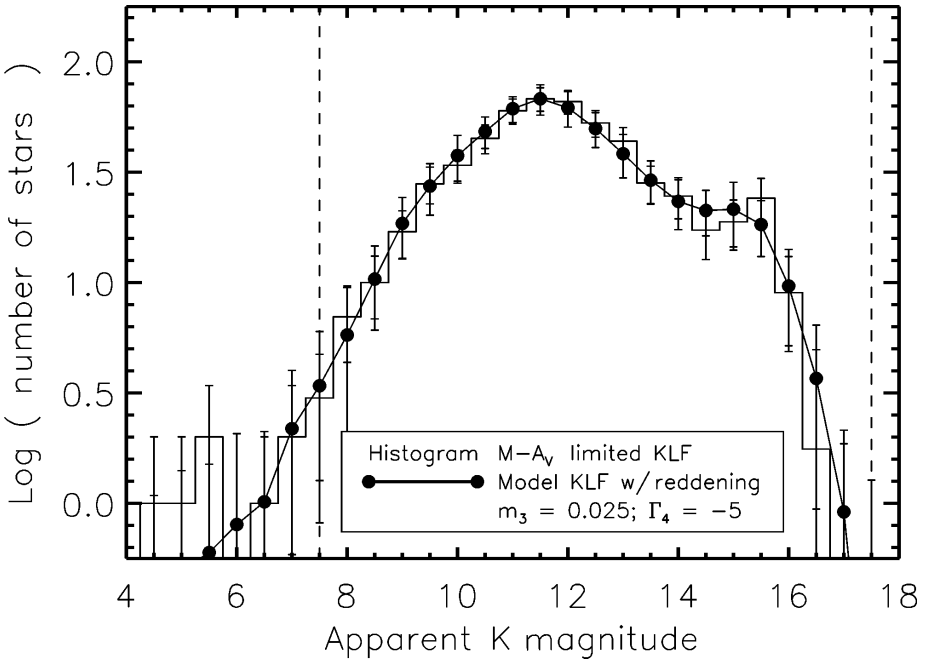

Figure 9 The K-band (2.2 μm) monochromatic luminosity function (histogram) of the Trapezium cluster constructed from the deep infrared imaging observations shown in Figure 8. This is a background-corrected, extinction-limited KLF complete to a cloud depth of A_V = 17 mag for million-year-old stars with masses greater than $\sim$0.015 $M_\odot$. Also plotted is the model KLF (*line*) corresponding to the underlying IMF (Figure 10) whose KLF best fit the data. Taken from Muench et al. (2002).

approximately $m_K \sim$ 11–12 mag, where it flattens before clearly falling again to fainter magnitudes. A clear secondary peak is present at approximately 15 mag, which is well into the brown dwarf luminosity range. At lower luminosities, the KLF rapidly drops off.

Muench et al. (2002) derived the IMF of the Trapezium cluster by using a suite of Monte Carlo calculations to model the cluster's KLF. The observed shape of a cluster luminosity function depends on three parameters: the ages of the cluster stars, the cluster MLR, and the underlying IMF (i.e., Equation 1). With the assumptions of a fixed-age distribution, derived from the spectroscopic study of the cluster by Hillenbrand (1997), a composite theoretical MLR adopted from published PMS calculations (i.e., Bernaconi 1996, Burrows et al. 1997, D'Antona & Mazzitelli 1997, Schaller 1992), and an empirical set of bolometric corrections, Muench et al. varied the functional form of the underlying IMF to construct a series of synthetic KLFs. These synthetic KLFs were then compared to the observed Trapezium KLF in a chi-squared minimization procedure to produce a best-fit

IMF. As part of the modeling procedure, the synthetic KLFs were statistically corrected for both variable extinction and infrared excess by using Monte Carlo probability functions for these quantities derived directly from multicolor (JHK) observations of the cluster.

The best-fit synthetic KLF is plotted in Figure 9. The corresponding underlying mass function is displayed in Figure 10 in the form of a histogram of binned masses of the stars in the best-fit synthetic cluster. This model mass function represents the IMF of the young Trapezium cluster. The main characteristics of this IMF are 1. the sharp power-law rise of the IMF from $\sim$10 $M_\odot$ (OB stars) to 0.6 $M_\odot$ (dwarf stars) with a slope (i.e., $\beta = -1.2$) similar to that of Salpeter (1955); 2. the break from the single power-law rise at 0.6 $M_\odot$ followed by a flattening and slow rise reaching a peak at $\sim$0.1 $M_\odot$, near the HBL; 3. the immediate steep decline into the substellar or brown dwarf regime; and 4. the prominent secondary peak near 0.015 $M_\odot$ or 15 M_J (Jupiter masses) followed by a very rapid decline to lower masses beyond the deuterium burning limit (at $\sim$10 M_J).

The most significant characteristic of this IMF is the broad peak, extending roughly from 0.6 to 0.1 $M_\odot$. This structure clearly demonstrates that there is a characteristic mass produced by the star-formation process in Orion. In effect, the typical outcome of the star-formation process in this cluster is a star with a mass between 0.1 and 0.6 $M_\odot$. The process produces relatively few high-mass stars and relatively few substellar objects. Indeed, no more than $\sim$22% of all the objects formed in the cluster are freely floating brown dwarfs. The overall continuity of the IMF from OB stars to low-mass stars and across the HBL strongly suggests that the star-formation process has no knowledge of the physics of hydrogen burning. Substellar objects are produced naturally as part of the same physical process that produces OB stars (see also Muench et al. 2001; Najita, Tiede & Carr 2000).

In this respect, the secondary peak at 0.015 $M_\odot$ is intriguing. The existence of such a peak may imply a secondary formation mechanism for the lower-mass brown dwarfs, similar to suggestions recently advanced by Reipurth & Clarke (2000), and thus is potentially very important. However, the significance that should be attached to this feature depends on the accuracy of the adopted MLRs for substellar objects used in the modeling. These MLRs may be considerably more uncertain than those of PMS stars. Indeed, observations of an apparent deficit of stars in the M6–M8 range of spectral types in a number of open clusters are suggestive of the existence of a previously unknown opacity feature in the MLR for such cool stars (Dobbie et al. 2002). The presence of such a feature could produce a peak in the luminosity function and a corresponding artificial peak in the derived mass function if not included in the theoretical MLRs (e.g., Kroupa Tout & Gilmore 1990, 1993). Given that this spectral type range corresponds to the temperature range predicted for young low-mass brown dwarfs, it is quite plausible that the secondary feature in the derived IMF is artificial and does not represent a true feature in the underlying IMF. Clearly more data, both observational and theoretical, is needed to assess the reality and significance of this intriguing feature.

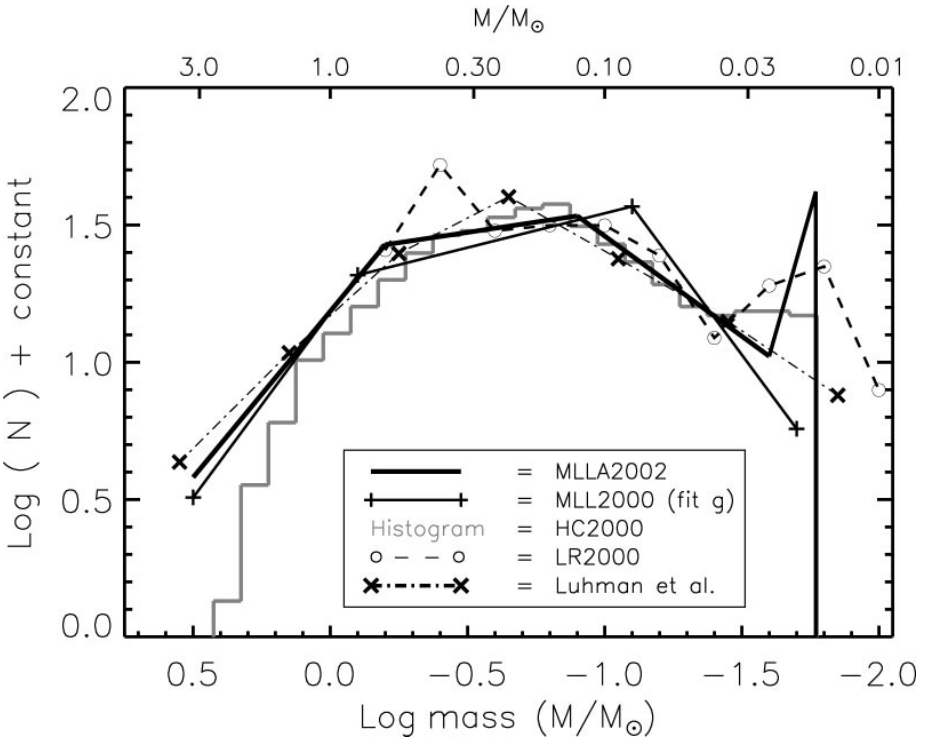

Figure 11 Comparison of IMFs derived from infrared observations reported in recent studies in the literature. These IMFs, derived from independent observations using a variety of techniques, are in very good agreement concerning the basic functional form of this cluster's IMF. In particular, all exhibit a broad peak extending from roughly 0.6–0.1 $M_{\odot}$ followed by a clear decline in the substellar regime. This suggests a characteristic mass is produced by the star-formation process.

Figure 11 shows a comparison of Trapezium IMFs recently derived from a number of different deep infrared imaging surveys using a variety of methods (Hillenbrand & Carpenter 2000; Lucas & Roche 2000; Luhman et al. 2000; Muench et al. 2000, 2003). The general agreement of the derived IMFs is impressive for $m_* > 0.015\ M_{\odot}$. The fundamental features (1–3) described above are evident in all the IMFs. In the region of the secondary peak (4), the agreement is less impressive, likely reflecting the inherent uncertainties in the modeling at the lowest substellar masses. Nonetheless, there is general agreement that the IMF turns over and falls off below the HBL and into the substellar mass regime. However, the precise details, such as the steepness of the falloff and the amplitude of the secondary peak, remain somewhat uncertain. Other differences in details between the various IMFs likely result from the uncertainties inherent in the different techniques used in the IMF determinations and provide some measure of the overall

uncertainty in our present ability to measure the exact form of the IMF in this cluster. Clearly, however, these infrared studies of the Trapezium cluster have established the fundamental properties of its IMF.

The derived IMF of the Trapezuim cluster spans a significantly greater range of mass than any previous IMF determination whether for field stars or other clusters (e.g., Kroupa 2002). Its statistically meaningful extension to substellar masses and the clear demonstration of a turnover near the HBL represents an important advance in IMF studies. For masses in excess of the HBL, the IMF for the Trapezium is in good agreement with the most recent determinations for field stars (Kroupa 2002). This is to some extent both remarkable and surprising because the field-star IMF is averaged over billions of years of galactic history, assuming a constant star-formation rate, over the age of the Galaxy and over stars originating from very different locations of galactic space. The Trapezium cluster, however, was formed within the past million years in a region considerably less than a parsec in extent. Moreover, there is evidence that this region is not yet finished producing stars, as significant star formation appears to be continuing in the molecular cloud behind the cluster (Lada et al 2000). Taken at face value, this agreement suggests that the IMF and the star-formation process that produces it is very robust, at least for stellar mass objects.

3.4. Comparison with Other Embedded Clusters: A Universal IMF?

Although few other embedded clusters have been as completely studied as the Trapezium, the luminosity and mass functions of a number of such clusters have been investigated in various levels of detail. These include clusters such as IC348 (Lada & Lada 1995; Luhman et al. 1998; Muench et al. 2003; Najita, Tiede & Carr 2000), NGC 1333 (Aspin, Sandell & Russell 1994; Lada, Alves & Lada 1996), NGC 2264 (Lada, Young & Greene 1993), NGC 2024 (Comeron et al. 1996, E.A. Lada et al. 1991b, Meyer 1996), Rho Ophiuchi (Bontemps et al. 2001, Comeron et al. 1993, Green & Meyer 1995, Lada & Wilking 1984), Serpens (Eiroa & Casali 1992, Giovannetti et al. 1998), M17 (E.A. Lada et al. 1991a), W3 (Megeath et al. 1996), and NGC 3603 (Brandl et al. 1999, Eisenhauer et al. 1998, Nurnberger & Petr-Gotzens 2002). Because of varying distances, sizes, sensitivities, and methodologies, these KLFs and corresponding IMFs were not uniformly sampled or investigated using a common systematic approach. As a result, only limited conclusions can be drawn from comparison of all these results with each other and with the IMF derived for the Trapezium cluster. However, when homogeneous data are analyzed with similar methodology, more meaningful comparisons of embedded cluster IMFs are possible (e.g., Lada et al. 1996, Luhman et al. 2000, Muench et al. 2002).

The first conclusion that can be drawn from such studies is that the KLF for embedded clusters is not a universal function and statistically significant variations are present in observed clusters (e.g., Lada, Alves & Lada 1996). This

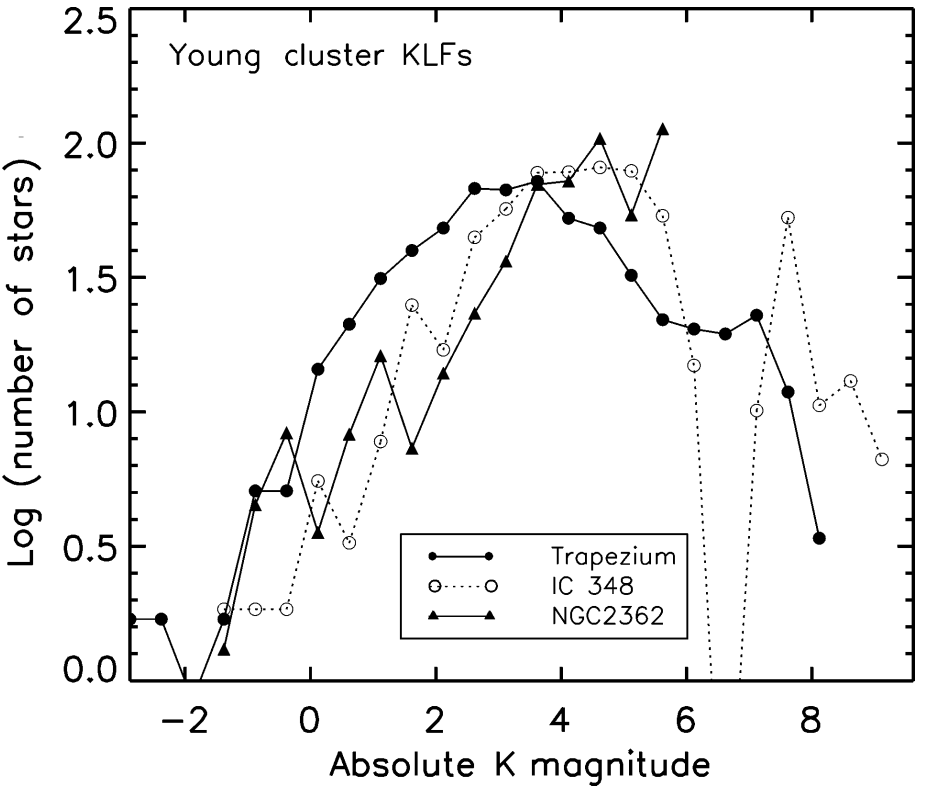

Figure 12 Comparison of the observed KLFs (adjusted to the same distance) of three young clusters of differing age: Trapezium (10^6 years), IC 348 (3×10^6 years), and NGC 2362 (5×10^6 years). A significant trend toward lower luminosity with age is apparent for these KLFs, similar to that predicted by evolutionary models (see Figure 13).

is illustrated in Figure 12, which displays the KLFs of the Trapezium, IC 348, and NGC 2362 clusters. Such variations in the cluster luminosity functions are not unexpected for embedded clusters that consist mostly of PMS stars. Even if such clusters were characterized by a universal IMF, they would experience significant luminosity evolution as their PMS population evolved and collectively approached the main sequence. This luminosity evolution would be particularly rapid during the first 5 Myrs of a cluster's existence, when the luminosities of its PMS stars experience their most rapid declines. For example, Figure 13 shows the expected KLFs for three different aged synthetic clusters with identical IMFs. Using Monte Carlo simulations, Muench et al. (2000) calculated these KLFs. The systematic evolution of the KLFs to lower brightness is clearly evident and certainly would be significant enough to be observable. Indeed, modeling of the KLFs of clusters such as IC 348, NGC 2362, and the Trapezium indicates that observed differences

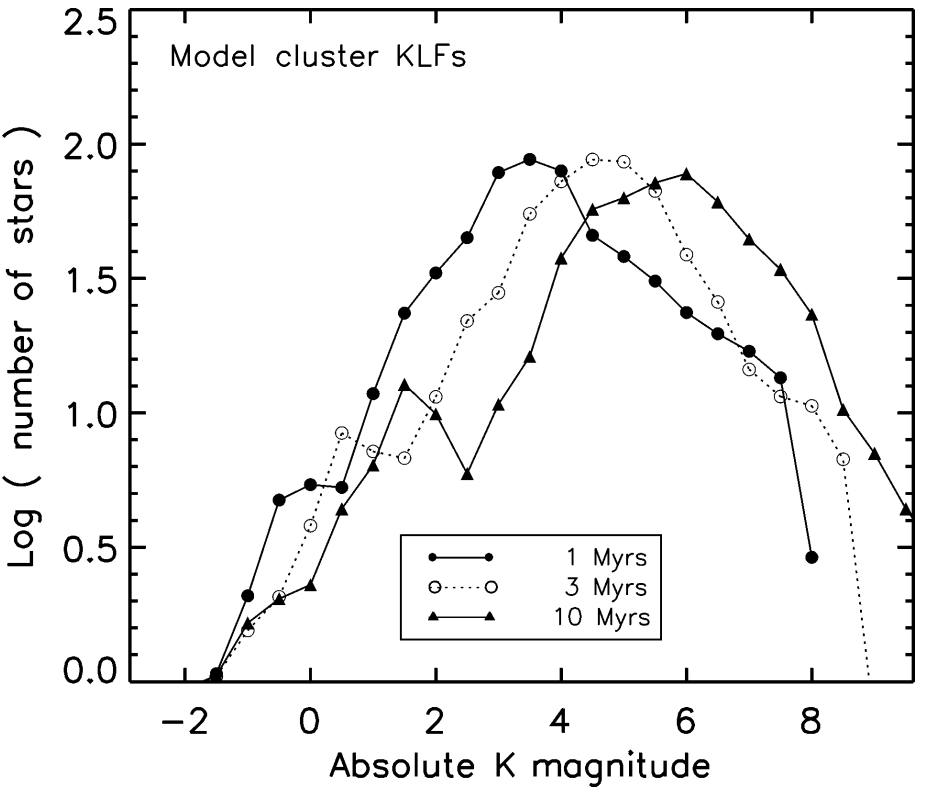

Figure 13 Model luminosity functions (KLFs) of synthetic clusters of differing ages but with the same underlying IMF (that of the Trapezium cluster). Young clusters experience systematic luminosity evolution, gradually becoming fainter with time, as PMS stars within them approach the main sequence. Figure prepared by A. Muench.

in their KLFs can be explained by the expected luminosity evolution in clusters that have very similar underlying mass functions (Alves et al. 2003, Lada & Lada 1995, Muench et al. 2002). This can also be inferred empirically, without resorting to modeling. Comparison of the KLFs of young clusters of known age shows that clusters of similar age display KLFs of very similar shape, whereas clusters of differing age show the greatest variation of KLF forms (Alves et al. 2003; Lada, Alves & Lada 1996).

To illustrate this further, we display in Figure 14 the background-corrected KLF and corresponding IMF derived for the IC 348 cluster from Monte Carlo modeling (Muench et al. 2003). IC 348 is the best-studied embedded cluster after the Trapezium. Although it is not as rich and suffers appreciably more background contamination, this cluster is closer to the solar system, older ($\tau \sim 2$–3 Myrs), and more evolved than the Trapezium cluster (Herbig 1998, Lada & Lada 1995). This

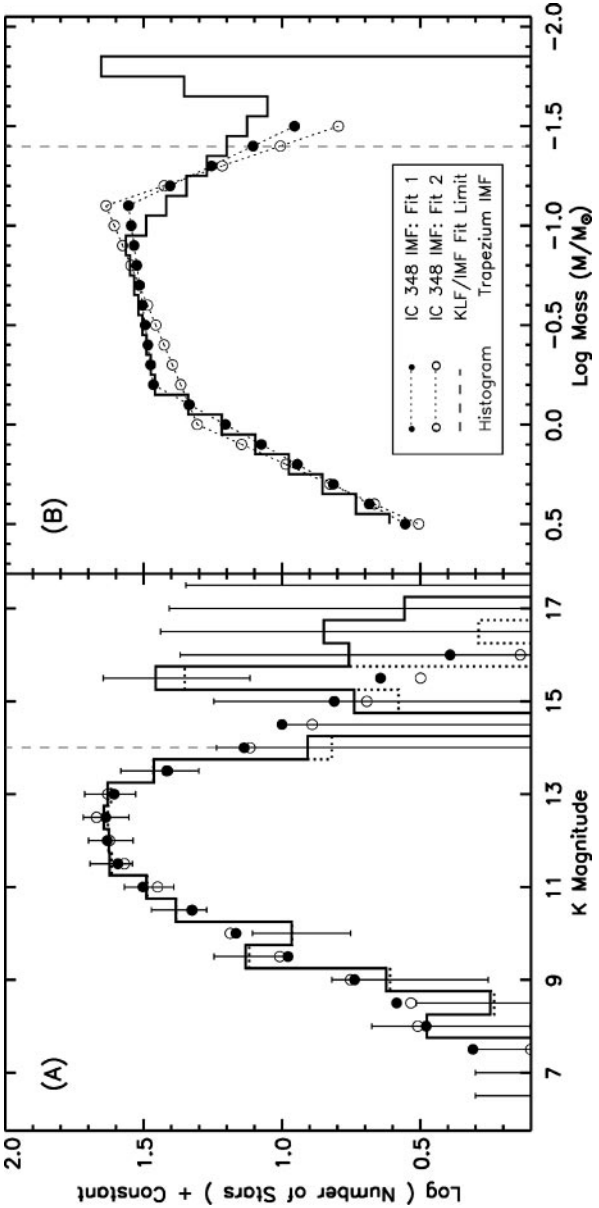

Figure 14 The KLF and derived IMF for IC 348. The left panel shows the observed background-corrected KLF (histogram of apparent magnitudes) along with the best-fit synthetic KLFs (*filled and open circles*) corresponding to the underlying model IMFs (*filled and open circles*) shown in the right panel. Also plotted is the IMF derived for the Trapezuim cluster. From Muench et al. (2003).

places additional constraints for IMF modeling, thus making the cluster a good candidate for comparison with the Trapezium. As seen in Figure 14, the IMF for this cluster derived from KLF modeling compares very well with that of the Trapezium over the entire range of mass ($m_* > \sim 15\ M_J$) over which it was determined. In particular, the IMF displays a broad peak between 0.1 and 0.5 $M_\odot$, with a clear turndown near the HBL. This indicates that there is a characteristic mass produced by the star-formation process in IC 348, and this mass is essentially the same as that suggested for star formation in the Trapezium. Moreover, the size of the substellar population of IC 348 is relatively well determined and constitutes only ∼25% of the cluster membership, again similar to the Trapezium. Because of poor statistics, Muench et al. (2003) did not fit the KLF in the luminosity range that corresponds to the location of the secondary peak in the substellar IMF of the Trapezium. However, examination of the IC 348 KLF shows a marginally significant bump at the luminosity corresponding to that mass. The relatively poor statistics in the IC 348 KLF at these faint magnitudes is due to a combination of the fact that IC 348 is not as rich as the Trapezium and it suffers more contamination from background stars because it is not foreground to a similarly opaque background molecular cloud.

Using independent observations and different methodology to extract IMFs from the observations, Luhman et al. (2000) derived IMFs for the Trapezium, IC 348, and Ophiuchi clusters and also found good agreement in the shapes of the IMFs of these clusters above the HBL. These comparisons again suggest a relatively robust or universal IMF. Another indication of the robustness of the IMF is found in the observations of NGC 3603, perhaps the most luminous and richest young cluster in the Galaxy. This distant (∼7 kpc), massive, and very dense OB star cluster contains low-mass (0.5–1 $M_\odot$) stars in roughly the proportion predicted for a normal IMF (Nurnberger & Petr-Gotzens 2002). This is interesting given the significant differences in cluster richness (and central densities) that likely correspond to differences in formation environment and internal star-formation rates. Indeed, it is entirely possible that the formation process for the Ophiuchi, NGC 1333, and, even perhaps, the Trapezium clusters is far from being completed. Yet, it seems that, once even 100 or so stars are formed, the fundamental form of the IMF is already determined. Differences in the underlying IMFs of these clusters may exist, but they are not large enough to be detectable given the existing uncertainties in the measurements that are likely dominated by the small sizes of the existing samples.

It is interesting that, as discussed above, a consensus that IMFs for open clusters can also be described by a universal form similar to the field-star IMF appears to be building (Massey 1998, Kroupa 2002). Here, we note that recent studies of the Pleiades (Adams et al. 2001, Bouvier et al. 1998) and α Per (Barrado y Navascues et al. 2002) clusters have extended the IMFs of these older (10^8 Myrs) clusters to the substellar regime; thus, an initial comparison can be made with the embedded clusters. These open cluster IMFs display the same four fundamental characteristics described above for the Trapezium cluster, including a secondary

peak in the low-mass portion of the substellar IMF. The IMFs do, however, differ in the location of the substellar peak. In the two older open clusters, this peak is found between 40 and 50 M_J, a significantly higher mass than suggested by observations of the Trapezium and IC 348 clusters ($\sim$15 M_J). This perhaps indicates that the feature is indeed the result of a hitherto unknown feature in the brown dwarf MLR (Dobbie et al. 2002) (discussed above).

Strong similarities have emerged in the IMFs derived for field stars, open clusters, and embedded clusters, thus suggesting a robust and universal IMF. However, there is some evidence that this universal IMF may not characterize all star-formation events. For example, *HST* observations of the extragalactic starburst cluster R136 (30 Dor) in the Large Magellanic Cloud suggest that the IMF of this O star–rich cluster flattens and departs from a Salpeter-like power-law rise at a mass of $\sim$2 $M_\odot$ (Sirianni et al. 2000). This is higher than the mass ($\sim$0.6 $M_\odot$) of the corresponding inflection point in the Trapezium, open cluster, and field-star IMFs and suggests a relative deficit of lower-mass stars in this rich O cluster. However, it is likely that the numbers of solar mass stars in R136 has been underestimated owing to the severe crowding in the cluster center. Even in this cluster, which contains 1000 O stars, the underlying IMF may quite possibly be characterized by the same universal form as that derived for the Trapezium. A more significant indication of a departure from a universal IMF may be present in recent observations of the nearby Taurus clouds. Luhman (2000) has found a significant (factor of two) deficit of substellar mass objects in this region, relative to the embedded population in the Trapezium and IC 348 clusters. The embedded population of the Taurus clouds is an embedded T association consisting of isolated stars and small loose groupings of stars formed over a relatively large area. These conditions are decidedly different from those that characterize embedded cluster formation. Because the IMF above the HBL for Taurus appears to be similar to that of clusters and the field (e.g., Kenyon & Hartmann 1995), the finding of a deficit of brown dwarf stars may indicate that the substellar IMF is less robust than the stellar IMF and thus may be a sensitive function of formation environment and/or initial conditions. However, more observations are necessary to test the significance of this possibility.

4. LABORATORIES FOR STAR AND PLANET FORMATION

Nearly half a century ago, Walker's (1956) observations of the partially embedded cluster NGC 2264 showed that its late-type (i.e., F and later) stars were characterized by subgiant luminosities that placed them well above the main sequence on the HRD. Thus, these observations empirically established the PMS, pre–hydrogen burning, nature of young low-mass stars and provided the critical data needed to test and constrain the theory of PMS evolution (e.g., Hayashi 1966). Thirty years later, infrared observations of the embedded cluster in Ophiuchus enabled the first systematic classification of infrared protostars and young stellar objects on the basis of emergent stellar energy distributions (Lada 1987, Lada & Wilking 1984,

Wilking & Lada 1983). Such observations were very influential in constructing the early framework for a theoretical understanding of low-mass star formation (e.g., Shu, Adams & Lizano 1987). Today, embedded clusters continue to play an important role in the development and testing of theories dealing with the formation and early evolution of both stars and planetary systems.

4.1. Protostars and Outflows

Embedded clusters contain young stellar objects in various evolutionary states, including deeply buried protostars with their infalling envelopes and associated bipolar outflows as well as more exposed PMS stars surrounded by protoplanetary accretion disks. Clusters are particularly useful for statistical studies of the evolution of such objects. For example, infrared photometric and spectroscopic observations have been used in comparative studies to investigate the physical and evolutionary natures of embedded populations in clusters. Observational investigations of the embedded Ophiuchi cluster led to the identification of four classes of young stellar objects corresponding to four phases of early stellar evolution (Adams, Lada & Shu 1987; Andre, Ward-Thompson & Barsony 1993; Lada & Wilking 1984). The ratios of the numbers of objects in the various stages coupled with cluster ages have led to estimates for the lifetimes of the various states of early stellar evolution. For example, the rarity of protostars in even the youngest clusters suggests that the protostellar phases are relatively short, $\sim 10^4$ years to $\sim 10^5$ years (e.g., Andre & Montmerle 1994; Greene et al. 1994; Wilking, Lada & Young 1989). Coupled with observation of source luminosities and estimates of the masses of the underlying stars, these timescales yield mass accretion rates for protostellar evolution that constrain theoretical predictions (Shu, Adams & Lizano 1987).

More recently, spectroscopic surveys of embedded clusters have been employed to systematically investigate the more detailed physical properties of embedded populations. Low-resolution infrared spectroscopic surveys of the embedded population in the Rho Ophiuchi cluster revealed significant differences between protostellar objects and PMS stars, thus indicating that protostellar photospheres were heavily veiled. The large measured veilings are likely the result of excess emission originating in infalling envelopes and surrounding accretion disks (Casali & Eiroa 1996, Casali & Matthews 1992, Greene & Lada 1996). Deep, high-resolution spectral observations of the embedded populations of the Ophiuchi cluster further found the rotation rates of classical protostars (Class I sources) to be systematically greater than those of disk-bearing PMS stars (Class II sources) in the cluster, which suggests that rotation rates in young stellar objects may be modulated by their accretion rates (Greene & Lada 1997, 2002).

The demographics of the protostellar populations in embedded clusters are not well known and are poorly constrained by existing observations. Although generally rare, protostars are most abundant in the youngest embedded clusters where as many as 15–20% of the members can be protostellar in nature. Examples

of embedded clusters that are protostar rich include NGC 1333, Serpens, and Rho Ophiuchi. Likely no more than 10^6 years old, these clusters represent the least-evolved embedded clusters known. Indeed, NGC 1333 and the Serpens cluster each contain relatively large populations of Class 0 sources, the most deeply embedded and least-evolved protostellar class identified (Sandell & Knee 2001, Hurt & Barsony 1996). These two clusters are also rich in bipolar outflows, and both appear to be undergoing recent bursts in outflow activity (Bally, Devine & Reipurth 1996; Davis et al. 1999; Knee & Sandell 2000). Both NGC 1333 and Serpens are experiencing vigorous star formation and likely are true protoclusters, still largely in the process of being constructed from molecular gas and dust. This is in contrast to the situation for older embedded clusters such as IC 348, which at an age of $\sim$2–3 Myrs appears to have few protostellar sources and only one outflow (Lada & Lada 1995; McCaughrean, Rayner, & Zinnecker 1994). Lada et al. (1996) have argued that NGC 1333 and IC 348 have similar present-day rates of star formation and have suggested that NGC 1333 would evolve into a cluster similar to IC 348 if star formation were to continue in NGC 1333 at the same rate for another 2–3 Myrs. However, once a cluster's age exceeds the timescale ($\sim 10^5$ years) for protostellar evolution, then the older and more evolved the cluster becomes, the smaller the fraction of protostars and outflows it will contain (e.g., Fletcher & Stahler 1994b). Because most embedded clusters have ages between 1 and 3 Myrs, their membership is typically dominated by PMS stars.

4.2. Circumstellar-Protoplanetary Disks

PMS stars come in two varieties: those with circumstellar disks (Class II) and those without such disks (Class III). The frequency of disks within a cluster is directly related to the physical processes of disk formation and evolution. Because circumstellar disks can be the progenitors of planetary systems, knowledge of the cluster disk fraction (CDF) and how it evolves with time have important consequences for understanding the origin of planetary systems. Because most stars probably formed in embedded clusters, the measurement of the CDF in the youngest embedded clusters produces a determination of the initial disk frequency (IDF), which in turn directly measures the probability of disk formation around newly formed stars. Coupled with knowledge of the probability of planet formation in circumstellar disks, the IDF can provide an estimate and indirect census of extrasolar planetary systems in our galaxy. The variation of the CDF with cluster age sets the timescale for disk evolution and thus the duration or lifetime of the circumstellar disk (and planet building) phase of early stellar evolution. This therefore provides a critical constraint for determining the probability of planet formation in circumstellar disks and also directly bears on the question of the ubiquity of extrasolar planetary systems. Do stars of all masses form with circumstellar disks? Is the likelihood of forming planetary systems from disks dependent on the mass of the central star, on the environment in which the star formed, or on both? These and similar questions

concerning the origins of planetary systems may be best addressed by observations of embedded clusters.

The CDF and its dependence on stellar mass and cluster age, in principle, can be directly measured by obtaining the infrared spectral energy distributions of all or a representative fraction of a cluster population. This is because stars with circumstellar disks emit excess infrared emission that displays a clear and specific spectral signature in the star's optical-infrared energy distribution (e.g., Adams, Lada & Shu 1987; Lynden-Bell & Pringle 1974). In practice, it is prohibitive to obtain complete (i.e., 1–1000 μm) infrared spectral energy distributions of a cluster population because to do so requires multiwavelength ground-based and space-based observations. However, an infrared excess from a disk can be measured at any infrared wavelength sufficiently longward of the peak of the underlying stellar energy distribution of the central star. Although, the longer the wavelength the more unambiguous the infrared excess, observations at wavelengths as short as 2 μm (K band) can detect infrared excesses in the majority of disk bearing stars. Indeed, essentially all stars with circumstellar disks containing 10^{-9} $M_{\odot}$ of hot dust or more can be detected using ground-based L-band (3.4 μm) observations (Lada et al. 2000, Wood et al. 2002).

Near-infrared JHK imaging surveys of numerous embedded clusters have suggested that the IDF is relatively high $>50\%$ (e.g., Carpenter et al. 1997; Lada, Alves & Lada 1996; Stauffer et al. 1994). Indeed, longer wavelength (i.e., 3–10 μm) surveys, which are more sensitive to disk excess emission, have determined IDFs of $\sim$80–85% for the Trapezium (Lada et al. 2000) and NGC 2024 (Haisch, Lada & Lada 2000; Haisch et al. 2001c) clusters in Orion, two of the youngest clusters studied. These results suggest that circumstellar disks are a natural byproduct of the star-formation process and that most stars, independent of mass, are therefore born with the ability to form planetary systems.

However, infrared studies of embedded populations and clusters have also suggested that the duration of the accretion or protoplanetary disk phase may be relatively brief (3–15 $\times$ 10^6 years) (Brandner et al. 2000; Lada & Lada 1995; Skrutskie et al. 1990; Strom, Edwards & Skrutskie 1993; Strom et al. 1989). Because the building times for giant gaseous planets are estimated to be 10^7 years or longer (Lissauer 2001), it is critically important to accurately constrain the empirical disk lifetime measurements. Young clusters offer an excellent laboratory for investigating disk evolution timescales. These clusters present statistically significant samples of stars whose mean ages are well determined. Moreover, by combining observations of embedded as well as revealed clusters, one can create a sample that spans a range in age much greater than that characterized for any individual star-forming region. Recently, Haisch, Lada & Lada (2001a) performed the first systematic and homogeneous observational survey for circumstellar disks in young clusters. They used J-, H-, K-, and L-band (1.25 μm, 1.65 μm, 2.2 μm, and 3.4 μm, respectively) imaging observations to determine the CDF in six clusters whose ages varied between 0.3 and 30 Myrs. Figure 15 shows the CDF of their sample along with CDF measurements for two embedded T associations

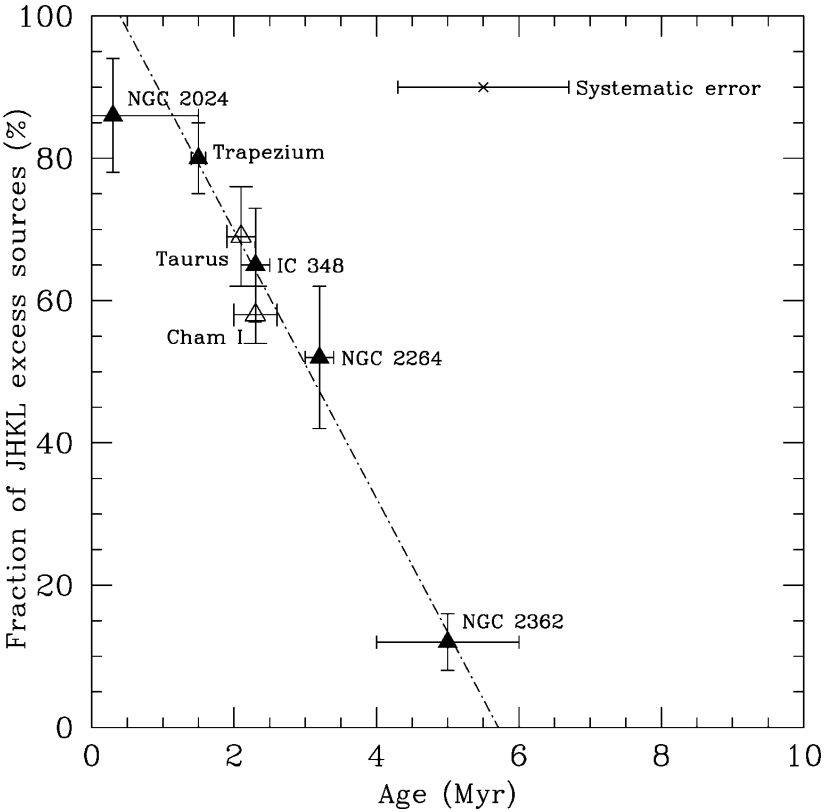

Figure 15 Disk fraction as a function of cluster age for a sample of young clusters with consistently determined mean ages. The disk fraction is initially very high but then rapidly drops with cluster age, suggesting maximum disk lifetimes of less than 6 Myrs in young clusters (Haisch et al. 2001a).

[Taurus (Kenyon & Hartmann 1995) and Chamaeleon I (Kenyon & Gomez 2001)]. The observations show a rapid decline in the CDF with cluster age. Half the disks in a cluster appear to be lost within only 2–3 Myrs, and essentially all the disks are gone in approximately 5–6 Myrs. Moreover, observations also indicate that disk lifetimes are also functions of stellar mass, with disks around higher-mass stars evolving more rapidly than disks around low-mass stars (Haisch, Lada & Lada 2001b). Such a rapid timescale for disk evolution places stringent constraints on the timescale for building planets, particularly giant gaseous planets.

However, the JHKL observations of Haisch et al. (2001a) trace the infrared excess arising from small (micron-sized), hot (900-K) dust grains located in the inner regions of a circumstellar disk ($\sim$0.25 AU). It is possible for substantial amounts of material to still be present in the disk if either this material is purely gaseous or the disk has a large inner hole. The former situation could arise if significant

grain growth occurs as a result of dust settling and rapid grain coagulation and growth, as is the expected first step in the formation of planetesimals. However, any turbulence in the disk would be expected to keep detectable amounts of small dust grains suspended within the gas (Ruden 1999), so dust should still remain a good tracer of total disk mass as the disks evolve. Indeed, recent observations of dust and H_2 emission in more-evolved and much less-massive debris disks appear to support this assumption (Thi et al. 2001). The latter possibility could occur if protoplanetary disks evolved large inner holes as they aged. It has been noted that in the Taurus clouds near-infrared L-band excess is closely correlated with millimeter-continuum emission, which traces outer disk material, thus suggesting that the evolution of the inner and outer disks is homologous and occurs on the same timescale (Haisch et al. 2001b). Similarly, a recent millimeter-continuum survey of four young embedded clusters (NGC 2071, NGC 2068, NGC 1333, and IC 348) has found that the variation in the fraction of detected millimeter sources from cluster to cluster is similar to the variation in the fraction of near-infrared excess sources (E.A. Lada, K.E. Haisch, S.V.W. Beckwith, unpublished manuscript). This implies that the lifetimes of the inner disk, as detected by near-infrared excess, and the outer disk, as detected at millimeter wavelengths, are coupled for embedded clusters as they were for the Taurus population. These observations strengthen the previous L-band excess determination of a short disk lifetime of <6 Myrs and further suggest that the lifetime for massive outer disks may be as long as only 3 Myrs. Indeed, the dearth of strong millimeter-continuum emission from the disk population of the very young Trapezium cluster implies even more rapid outer-disk evolution (Bally et al. 1998; Lada 1999; Mundy, Looney & Lada 1995). Disk lifetimes may also depend on internal cluster environment (e.g., the degree to which a cluster produces O stars). Systematic surveys of a larger population of clusters are needed to assess this possibility. In particular, mid-infrared surveys that will be carried out by the SIRTF mission should more definitively address this question.

4.3. Brown Dwarfs

As discussed above, embedded clusters contain significant populations of substellar objects. Indeed, the Trapezium cluster alone contains nearly as many brown dwarfs as have been identified in the galactic field to this point in time. However, in the two clusters (Trapezium and IC 348) with the most complete substellar census, substellar objects account for only approximately 20–25% of the total cluster population. Thus, if embedded clusters such as these supplied the galactic field population, then we would expect to find only one brown dwarf for every three to four stars in a typical volume of Galactic space. Embedded cluster research has provided one of the most interesting discoveries concerning the nature of brown dwarfs. Examination of young brown dwarfs and brown dwarf candidates in a number of embedded clusters, including IC 348, Ophiuchus, and the Trapezium, and in other star-forming regions, such as the Chamaeleon Clouds, has produced evidence that some brown dwarfs emit excess emission at near- and mid-infrared

wavelengths similar to that emitted by stars with circumstellar disks (e.g., Luhman 1999, Nata & Testi 2001, Natta et al. 2002, Wilking et al. 1999). Moreover, deep near-infrared images of the Trapezium have enabled the first statistically significant determination of the disk frequency for an embedded substellar population. Muench et al. (2001) found that a very high fraction (65%) of the substellar objects in the cluster display infrared excess emission at 2 μm, suggestive of the presence of circumstellar disks. Moreover, Muench et al. (2001) discovered that approximately 20% of the substellar population were optical proplyds on *HST* archive images, independently confirming the presence of circumstellar disks around a significant fraction of the substellar objects in the cluster. Because observations of 2-μm excess undercount disk-bearing stars, the actual fraction of substellar objects with disks is likely greater than 65% and thus very similar to the disk fraction (80%) observed for the stellar population of the cluster (Lada et al. 2000). Like stars, brown dwarfs appear to be formed surrounded by disks and as a result possess the ability to form planetary systems. The detection of infrared excess around the faintest sources in the KLF of the Trapezium cluster also conclusively established the nature of these sources as young objects and cluster members and thus confirmed their status as bona fide substellar objects. Furthermore, the detection of a high disk fraction (similar to that of the stellar population) coupled with the smooth continuity of the IMF across the HBL provides strong evidence that freely floating brown dwarfs are a natural product of the star-formation process in embedded clusters. The formation process for brown dwarfs is essentially identical to that of stars.

4.4. Binary Stars

Because most field stars appear to be binary systems, understanding the origin of binary star systems is of fundamental importance for developing a general theory of star formation. Clusters are important laboratories for investigating binary formation and evolution. In this context, it is interesting that the binary fractions of well-studied embedded clusters such as the Trapezium (Petr et al. 1998; Prosser et al. 1994; Simon, Close & Beck 1999), IC 348 (Duchene, Bouvier & Simon 1999), and Rho Ophiuchi (Simon et al. 1995) are found to be indistinguishable from that of the galactic field. However, it is well established that the binary fraction of the embedded population in the Taurus-Auriga association is significantly (a factor of two) in excess of that of the galactic field (e.g., Duchene 1999; Ghez, Neugebauer & Matthews 1993; Leinert et al. 1993). This difference in binary fraction provides an important clue relating to the origins of galactic field stars. Specifically, it supports the notion that most field stars originated in embedded clusters rather than in embedded associations such as the Taurus-Auriga clouds.

However, it has been suggested that the Taurus-Auriga binary fraction may represent the initial binary fraction even for stars that form in embedded clusters. Kroupa (1995a,b) performed N-body experiments to simulate the evolution of a binary population in a young cluster. These experiments began with clusters

containing 100% binaries and showed that stellar encounters could disrupt binaries and reduce the overall binary fraction with time. Moreover, Kroupa found that the field-star binary population could be produced by such a model, if most stars formed in what he identified as a dominant-mode cluster, i.e., a cluster with roughly 200 stellar systems and a one-half mass radius of 0.8 pc. The fact that such clusters are relatively common (e.g., Table 1) lends support to this notion. Furthermore, the concept that disruption of multiple systems can occur in clusters appears to be supported by the observation of a deficit of wide binaries in the Trapezium cluster (Scally, Clarke & McCaughrean 1999). However, the binary fraction of embedded clusters is not significantly different from that of much older open clusters (Patience & Duchene 2001). This indicates that any evolution of the binary fraction must have occurred on timescales on the order of 1 Myrs or less. Such rapid evolution in the binary population can occur for a very dense embedded cluster such as the Trapezium (Kroupa, Aarseth, & Hurley 2001; Kroupa, Petr & McCaughrean 1999). It is not clear, however, whether binaries can be as efficiently disrupted in the lower-density clusters that account for most star formation. The question of a universal initial binary fraction remains open. Star formation may produce a variety of outcomes for the emerging binary fraction owing to a corresponding variety of initial conditions. Determinations of the binary properties of the protostellar populations in embedded clusters could provide an important test of this question. If there is a universal initial binary fraction, then essentially all protostellar objects must be nascent binary systems. High-resolution infrared imaging and spectroscopic monitoring of Class I sources in embedded clusters could resolve this issue.

5. ORIGIN AND DYNAMICAL EVOLUTION

5.1. Formation of Embedded Clusters

To understand how an embedded cluster forms, we must understand two basic physical processes: 1. the formation of a massive, dense core in a GMC and 2. the subsequent development of stars from dense gas in the core. Molecular clouds form from the turbulent, diffuse, and atomic interstellar medium by a physical process or collection of processes that are not well understood. Overall this process likely involves the complex interplay of things such as spiral density waves, supernova explosions, the galactic dynamo, phase transitions, and various types of instabilities (e.g., thermal, gravitational, magneto-hydrodynamic, etc.) (e.g., Elmegreen 1991, 1993). The vast majority of GMCs are observed to contain dense gas and signposts of star formation, which suggests that the formation of dense cores and then stars proceeds very rapidly after the cloud has formed from the diffuse interstellar medium. The GMCs that form from the ISM are gravitationally bound entities with highly supersonic and turbulent velocity fields. The turbulent dissipation timescales for GMCs are thought to be shorter than the cloud lifetime, suggesting that on global scales the clouds are stabilized against collapse by internal turbulent pressure.

Numerical simulations (e.g., Klessen, Heitsch & Mac Low 2000) suggest that under such conditions supersonic turbulent flows can collide, shock, and dissipate energy. Under the right conditions, these collisions can produce dense cores that are gravitationally unstable and can decouple from the overall turbulent flow. The largest and most massive of these fragments are the potential sites of cluster formation.

The second step of the cluster formation process is the rapid evolution of dense gas in a massive core to form stars. This likely involves the continued dissipation of turbulence in the dense gas that is followed by fragmentation, gravitational instability, and the formation of protostellar seeds, which grow by accreting their infalling envelopes and then perhaps other surrounding dense gas from the general potential in which they are embedded (e.g., see reviews by Clarke et al. 2001, Elmegreen et al. 2001). This scenario appears to be quite different from that which has successfully explained the formation of isolated low mass stars from individual low-mass cores. Such solitary stars form from initially turbulent, magnetically supported, dense cores that evolve through ambipolar diffusion of magnetic fields to be dynamically unstable and then collapse from the inside out (Shu, Adams & Lizano 1987). The cores that form isolated low-mass stars in this manner have sizes that are considerably larger than the separation of stars in an embedded cluster. Evidently, protostellar cores in clusters must have smaller radii than those which form in isolation. This suggests that cluster-forming cores must experience significant fragmentation in their evolution to form stars. The physical mechanism that produces this fragmentation is not well understood. This process likely involves progressive cooling of a marginally stable or collapsing massive core that continuously reduces the Jean's mass. In turbulent dense cores, this cooling takes place as a result of dissipation or loss of turbulence. An elegant possibility to account for fragmentation was proposed by Myers (1998) for the case of magnetohydrodynamics (MHD) turbulence. If the ionization rate in a massive core is low enough (i.e., the extinction is high enough that cosmic rays are the sole source of ionization), then MHD waves greater than a certain frequency cannot couple well to the neutral gas. This corresponds to a cutoff wavelength, below which turbulence can no longer be sustained (e.g., Mouschovias 1991). This situation can lead to the formation of a matrix of critically stable Bonnor-Ebert condensations or kernels confined by the pressure in the surrounding gas. Myers (1998) found that for typical conditions the sizes of these kernels can be comparable to the separation of stars in embedded clusters. Fragmentation can also be produced in the turbulent decay process as flows collide and shock, creating density enhancements, which, if massive enough, can become gravitationally bound and will separate from the general turbulent velocity field (e.g., Klessen & Burkert 2000, 2001). Once these fragments or kernels become gravitationally unstable, they collapse. Gaining mass through infall of surrounding material, they will become protostars. However, the rates at which protostellar condensations grow must vary significantly within the cluster. This is because the star-formation process must produce a range of stellar and substellar masses spanning three orders of magnitude within a timescale

of only a few (1–2) million years to reproduce the stellar IMF. As they move through the cluster core, protostellar fragments also accrete additional material from the reservoir of residual gas that is not locked up in other protostellar objects (Bonnell et al. 2001a). Because all these stellar embryos share a common envelope, a process of competitive accretion begins with initially more massive protostellar clumps or clumps closer to the center of the cluster experiencing higher accretion rates. The process is highly nonlinear and, even for a cluster with initially equal mass protostellar fragments, can lead to the development of a protostellar mass spectrum similar to that of the stellar IMF (Bonnell et al. 2001b, Klessen 2001). In this picture, the more massive stars tend to be formed in the central regions of the cluster, leading to some degree of primordial mass segregation. It is also possible for protostellar fragments in the dense inner regions of the cluster to collide and coalesce, leading to the production of very massive stars (Bonnell, Bate & Zinnecker 1998). It would otherwise be difficult to build up a massive star from general accretion because radiation pressure from embryonic stars more massive than approximately 10 $M_{\odot}$ can reverse infall and stunt the growth of the star (e.g., Adams, Lada & Shu 1987).

As indicated in Table 1, embedded clusters span a range in mass of at least two orders of magnitude. Yet their ages are all probably within a factor of two of 2 Myrs. This fact suggests that the star-formation rates in clusters vary widely. This is even more apparent when one considers the more distant "starburst" clusters such as NGC 3603 and R 136 that contain almost as many O stars as the entire memberships of embedded clusters such as NGC 1333 and Ophiuchi. Yet all these clusters are likely to be within a factor of two of the same age. The finding of a significantly higher star-formation rate for the Trapezium cluster compared to that in the two embedded clusters (IC 348 and NGC 1333) in the Perseus molecular complex led Lada et al. (1996) to suggest that the star formation in the Trapezium cluster was externally triggered. Compressive triggering increases the external pressure, and thus the density of a core, and in doing so speeds up the star formation. The close association of other clusters with adjacent HII regions has also suggested that triggering may have played an important role in the formation of at least some clusters [e.g., S 255 (Howard et al. 1997), S 281 (Megeath & Wilson 1997), W3–W4 (Carpenter et al. 2000)]. At some point, when molecular gas is either depleted or expelled from the cluster, star formation ceases and the cluster emerges from its molecular womb.

5.2. Emergence from Molecular Clouds: Dynamical Evolution and Infant Mortality

Although the origin of embedded clusters remains a mystery, the subsequent dynamical evolution of embedded clusters and their emergence from molecular clouds are well-posed theoretical problems that have been studied extensively both analytically (e.g., Elmegreen 1983, Hills 1980, Verschueren & David 1989) and numerically (Geyer & Burkert 2001; Goodwin 1997; Kroupa, Aarseth & Huley

2001; Kroupa & Boily 2002; Lada, Margulis & Dearborn 1984). As described above, clusters form in massive dense cores of molecular gas that are strongly self-gravitating. Star formation is an inherently destructive process for the GMC, and upon formation, new stars will immediately begin to disrupt their surrounding gaseous environments. The birth of high-mass stars can be particularly destructive and leads not only to the rapid disruption of a cluster-forming core, but also to the complete dispersal of an entire GMC (e.g., Whitworth 1979). Moreover, outflows generated by a population of low-mass stars are also capable of disrupting a massive cloud core in a relatively short time (e.g., Matzner & McKee 2000). For example, Figure 16 shows a deep infrared image of the massive molecular cloud core containing the young, deeply embedded protocluster cluster NGC 1333. Here, numerous jets, visible in the image, and outflows generated by low-mass protostars have already significantly altered the structure of the star-forming cloud core. As a result of these effects, star formation is a relatively inefficient process. The gravitational glue that binds the system of stars and gas in an embedded cluster may be largely provided by the gas. Stars are then expected to orbit in a deep potential well of the dense core with orbital velocities (i.e., $\sigma \approx (G[M_{stars} + M_{gas}]/R)^{0.5}$) characteristic of the virial velocities of the dense gaseous material. As it emerges from a cloud, the evolution of an embedded stellar cluster is consequently sensitively coupled to the evolution of its surrounding gas.

The two physical parameters that determine the evolution of an emerging embedded cluster are the SFE and the timescale of gas dispersal from the cluster. The SFE [SFE $= M_{stars}/(M_{gas} + M_{stars})$] is a fundamental parameter of both the star- and cluster-formation processes. Because the measurement of the SFE requires a reliable and systematic determination of both the gaseous and stellar mass within a core, accurate SFE measurements are not generally available for cluster-forming regions. In Table 2, we list the SFEs for the sample of nearby embedded clusters (drawn from Table 1) that appear to be fully embedded and for which reasonable empirical determinations for the gaseous and stellar mass exist. The SFEs range from approximately 10 to 30%. These efficiencies are typical of those sometimes

TABLE 2 Star-formation efficiencies for nearby embedded clusters

Cluster name	Core mass ($M_\odot$)	Stellar mass ($M_\odot$)	SFE	References
Serpens	300	27	0.08	Olmi & Testi 2002
Rho Oph	550	53	0.09	Wilking & Lada 1983
NGC 1333	950	79	0.08	Warin et al. 1996
Mon R2	1000	341	0.25	Wolf et al. 1990
NGC 2024	430	182	0.33	E.A. Lada et al. 1991a,b
NGC 2068	266	113	0.30	E.A. Lada et al. 1991a,b
NGC 2071	456	62	0.12	E.A. Lada et al. 1991a,b

estimated for other embedded clusters, but they are also significantly higher than the global SFEs estimated for entire GMCs, which are typically only 1–5% (e.g., Duerr, Imhoff & Lada 1982). The fact that the clusters with the lowest SFEs (Serpens, Ophiuchi, NGC 1333) appear to be the least evolved suggests that the SFE of a cluster increases with time and can reach a maximum value of typically 30% by the time the cluster emerges from its parental cloud core. Whether all clusters can reach SFEs as high as 30% before emerging from a molecular cloud is unclear; however, it does seem apparent that clusters rarely achieve SFEs much in excess of 30% before emerging from molecular clouds.

The timescale for gas removal, τ_{gr}, from a cluster is even less well constrained by empirical data than by the SFE. However, the ultimate dynamical fate of an embedded cluster is determined by the relationship between τ_{gr} and τ_{cross}, the initial dynamical timescale of the cluster (i.e., $\tau_{cross} = 2R/\sigma$, where R is the radius and σ the velocity dispersion of the cluster). There exist two important dynamical regimes for τ_{gr} corresponding to explosive ($\tau_{gr} \ll \tau_{cross}$) and adiabatic ($\tau_{gr} \gg \tau_{cross}$) gas removal times. Typical embedded clusters are characterized by $\tau_{cross} \sim 1$ Myrs. Clusters that form O stars will likely remove any residual gas on a timescale shorter than this dynamical time. O stars can quickly ionize and heat surrounding gas to temperatures of 10^4 K causing an abrupt increase in pressure that results in rapid expansion of the gas. The expansion velocities are on the order of the sound speed in the hot gas and, for the dimensions of embedded clusters, correspond to gas removal timescales that can be as short as a few times 10^4 years. The dynamical response of the stars that are left behind after such explosive gas removal will depend on the SFE achieved by the core at the moment of gas dispersal. For the cluster to remain bound in the face of rapid gas removal, the escape speed from the cluster, $V_{esc} \approx (2GM/R)^{0.5}$, must be less than σ, the instantaneous velocity dispersion of the embedded stars at the time of gas dispersal. Thus a bound group will emerge only if the SFE is greater than 50% (Wilking & Lada 1983). Consequently, the fact that the SFEs of embedded clusters are always observed to be less than 50% is critically important for understanding their dynamical evolution. Apparently, it is very difficult for embedded clusters to evolve to bound open clusters, particularly if they form with O stars.

However, classical open clusters, like the Pleiades, do exist in sufficient numbers such that at least some embedded clusters with SFEs less than 50% must have evolved to become relatively long-lived, bound systems. For slow gas removal times, $\tau_{gr} > \tau_{cross}$, clusters including those with low SFEs can adiabatically adjust and expand to new states of virial equilibrium and remain bound. The fact that clusters older than approximately 5 Myrs are observed to rarely be associated with molecular gas suggests that $\tau_{gr} < 5$ Myrs. This is close enough to the crossing timescales so that numerical calculations are necessary to investigate the response of clusters to this slow gas removal. Moreover, to produce a bound group that is stable against galactic tides and the tidal forces of its parental GMC requires additional stringent constraints on the initial conditions prevailing in the cluster-forming cloud core and on τ_{gr} (Lada et al. 1984). To evolve to a bound cluster like

the Pleiades, the typical embedded cluster would have to have a gas removal time of at least a few (3–4) crossing times, which corresponds to a few million years for typical conditions. This timescale is of the same order as the cluster formation or gestation time and would require a cluster to lose mass while forming stars. Outflows generated by low-mass stars can remove gas during the star-formation process, and Matzner & McKee (2000) have shown that such outflows can completely disrupt cluster-forming cores for SFEs in the 30–50% range. Whether such outflow-driven mass dispersal can occur over as long a timescale as is required is not clear. This depends on the detailed star-formation history of the cluster, in particular the star-formation rate and its variation in time, and neither of these quantities is sufficiently well constrainted by existing observations.

Numerical calculations show that those embedded clusters that do evolve to bound systems in such a manner undergo significant expansion as they emerge from a cloud; consequently, one expects bound open clusters to have significantly larger radii than those of embedded clusters, as is observed. In addition, during emergence, clusters can expand for long periods before they reach a final equilibrium. The appearance of bound and unbound emerging clusters are indistinguishable for clusters with ages less than 10 Myrs. Numerical calculations also show that even clusters that can survive emergence from a molecular cloud as bound systems may lose 10–80% of their numbers in the process. The more violent the gas disruption is, the smaller the fraction of stars that are bound will be. However, even clusters that experience explosive loss of gas can leave behind bound cores containing 10–20% of the original stellar population (Lada et al. 1984, Kroupa & Boily 2002). Therefore, bound clusters, even with O stars, can be produced, provided that the progenitor embedded cluster was substantially more massive and dense than the surviving open cluster.

Kroupa & Boily (2002) have pointed out that classical open clusters such as the Pleiades and Praesepe are massive enough to have formed with O stars and have posited that Pleiades-like clusters formed from much more massive protoclusters, most of whose original members were lost in the emergence from molecular gas. Indeed, Kroupa, Aarseth & Hurley (2001) have identified the Trapezium-ONC cluster as such a possible proto-Pleiades system: The Trapezium cluster is likely the future bound remnant of the emerging, mostly unbound ONC cluster. However, such proto-Pleiades systems would need to initially contain $\sim 10^4$ stars, considerably more than today appear to actually be contained in the ONC (1700 stars) and RCW 38 (1300 stars), the richest clusters in Table 1. In addition, if most open clusters lost one half or more of their original stars upon emergence from a molecular cloud, it would be difficult to understand the similarity of the embedded cluster and open cluster mass functions as well as the similarity of the stellar IMFs of embedded and open clusters. Nonetheless, a number of very rich and massive ($10^{4-5} M_{\odot}$) clusters in the Large Magellanic Cloud are surrounded by halos of unbound stars that account for as much as 50% of their total masses (Elson et al. 1987). If galactic globular clusters formed in such a manner, the stars lost in their emergence from their parental clouds could account for all the Population II

field stars in the Galactic halo (Kroupa & Boily 2002). The numerical simulations appear to indicate that, under most conditions leading to the formation of bound clusters, a significant fraction of the initial stellar population of a protocluster will be lost. Clearly, more extensive observations of the near environments of emerging embedded clusters would be useful to ascertain and quantify better the extent of any distributed or extended halos of young stars around these objects. Such information would provide important constraints for future modeling of emerging clusters.

The production of a bound cluster from a dense cloud core clearly requires special physical conditions. Hence, this must be a rare occurrence. The observed low SFEs for embedded clusters can account for the high infant mortality rate of clusters inferred from the relatively large numbers and high birthrates of embedded clusters compared to classical open clusters. Most (∼90–95%) embedded clusters must emerge from molecular clouds as unbound systems. Only the most massive ($M_{EC} \geq 500\ M_{\odot}$) embedded clusters survive emergence from molecular clouds to become stable, open clusters. Thus, although most stars form in embedded clusters, these stellar systems evolve to become the members of unbound associations, not bound clusters. However, bound classical clusters form at a sufficiently high rate, such that, on average, each OB association (and GMC complex) probably produces one such system (Elmegreen & Clemens 1985) accounting for approximately 10% of all stars formed within the Galaxy (Adams & Myers 2001, Roberts 1957).

6. CONCLUDING REMARKS

The discovery of large numbers of embedded clusters in molecular clouds over the past 15 years has led to the realization that these young protoclusters are responsible for a significant fraction of all star formation currently occurring in the Galaxy. Embedded clusters may very well be the fundamental units of star formation in GMCs. Conceived in the mysterious physical process that transforms diffuse interstellar matter into massive and dense molecular cloud cores, embedded clusters are born at a rate that significantly exceeds that estimated for stable, classical open clusters. Evidently, the vast majority of embedded clusters do not survive their emergence from molecular clouds as bound stellar systems. Their high infant mortality rate is mostly the result of the low to modest SFE and rapid gas dispersal that characterizes their birth. There are more than 20 embedded clusters formed for every cluster born that ultimately evolves into a long-lived system like the Pleiades. As the primary sites of star birth in molecular clouds, embedded clusters are important laboratories for studying the origin and early evolution of stars and planetary systems. The fundamental properties of the Galactic stellar population, such as its IMF, its stellar multiplicity, and the frequency of planetary systems within it, are forged in embedded clusters. Although, observations over the past 15 years have clearly established the the central role of embedded clusters in the star-formation process, the fundamental parameters of these extremely young clusters are still very poorly constrained. In particular, the overall census of embedded clusters is

far from complete, even within 1 kpc of the sun. In addition, very little information exists concerning the ages of embedded clusters. Accurate information regarding the spatial sizes, number of members, masses, and distances for most embedded clusters is also lacking. Nonetheless, despite these deficiencies, studies of individual embedded clusters have provided new insights into fundamental astrophysical problems, such as determining the functional form and universality of the IMF, the frequency and lifetimes of protoplanetary disks, and the ubiquity and nature of brown dwarfs. However, to date, only a small number of such clusters have been studied in any detail. It remains to be determined whether the trends determined for this small sample are representative of the majority of embedded clusters and star-formation events in the Galaxy as a whole. For example, does the IMF of the Trapezium cluster truly represent a universal IMF? Is the fraction of freely floating brown dwarfs always approximately 20–25% of a cluster population? Is the circumstellar disk lifetime the same in all clusters?

Other important questions also remain open. Do the progenitors of bound open clusters ever contain O stars? How frequently do O stars form in embedded clusters? Is the primordial binary fraction the same for stars formed in and outside rich clusters? What is the most massive embedded cluster that can be formed from a GMC? How many such clusters exist in the Galaxy? What is the actual number of poor ($N_* < 35$) embedded clusters or stellar aggregates formed, and what is the fraction of all stars produced in such groups? Is the process that produces embedded clusters in any way related to that responsible for the formation of globular clusters? Resolving these issues will require an extensive effort in both observation and theory. Prospects for progress continue to be bright owing to the development of important new observational capabilities, which include wide-field infrared imaging and multiobject spectroscopy using large, ground-based telescopes, airborne, and space-based infrared imaging and spectroscopy provided by missions such as SOFIA, SIRTF, and NGST, and NIR and all sky surveys such as 2MASS and DENIS. Practically everything we know about embedded clusters we have learned in the past 15 years. It is difficult to predict but exciting to contemplate what will be learned in the next 15 years as a result of these new capabilities and the continued dedicated efforts of astronomers who work on these problems. However, whatever the outcome of such research, there can be little doubt that the result of these efforts will be to enrich our understanding of the star- and planet-formation processes in the universe.

ACKNOWLEDGMENTS

We are grateful to João Alves, Richard Elston, and August Muench for assistance in preparation of figures. We also thank August Muench and Richard Elston for many useful comments and criticisms of earlier versions of this manuscript. E.A.L. acknowledges support from a Presidential Early Career Award for Scientists and Engineers, NSF AST 9733367, and from NSF grant AST 0204976 to the University of Florida at Gainseville. Finally, we gratefully acknowledge the efforts of the many

researchers whose contributions have made this such an interesting and stimulating subject to review.

The *Annual Review of Astronomy and Astrophysics* is online at http://astro.annualreviews.org

LITERATURE CITED

Adams FC, Lada CJ, Shu FH. 1987. *Ap. J.* 312:788–806

Adams FC, Myers P. 2001. *Ap. J.* 533:744–53

Adams JD, Stauffer JR, Monet DG, Skrutskie MF, Beichman CA. 2001. *Ap. J.* 121:2053–64

Allen C, Poveda A. 1974. In *The Stability of the Solar System and of Small Stellar Systems*, ed. Y Kozai, pp. 239–46. Dordrecht: Kluwer

Alves JF, Lada CJ, Lada EA, Muench AA, Moitinho A. 2003. *Astron. Astrophys.* In press

Ambartsumian VA. 1954. *Contrib. Byurakan Obs.* 15:3

Andre P, Montmerle T. 1994. *Ap. J.* 420:837–62

Andre P, Ward-Thompson D, Barsony M. 1993. *Ap. J.* 406:122–41

Aspin C, Barsony M. 1994. *Astron. Astrophys.* 288:849–59

Aspin C, Sandell G, Russell APG. 1994. *Astron. Astrophys. Suppl.* 106:165–98

Baade W, Minkowski R. 1937. *Ap. J.* 86:119–22

Bally J, Devine D, Reipurth B. 1996. *Ap. J. Lett.* 473:L49–53

Bally J, Testi L, Sargent A, Carlstrom J. 1998. *Astron. J.* 116:854–59

Baraffe I, Chabrier G, Allard F, Hauschildt PH. 1998. *Astron. Astrophys.* 337:403–12

Baraffe I, Chabrier G, Allard F, Hauschildt PH. 2002. *Astron. Astrophys.* 382:563–72

Barrado y Navascues D, Bouvier J, Stauffer JR, Lodieu N, McCaughrean MM. 2002. *Astron. Astrophys.* 395:813–21

Barsony M, Schombert JM, Kis-Halas K. 1991. *Astron. J.* 379:221–31

Battinelli P, Capuzzo-Dolcetta R. 1991. *MNRAS* 249:76–83

Bernasconi PA. 1996. *Astron. Astrophys. Suppl.* 120:57–61

Binney J, Tremaine S. 1987. *Galactic Dynamics*. Princeton, NJ: Princeton Univ. Press

Blaauw A. 1964. *Annu. Rev. Astron. Astrophys.* 2:213–46

Blitz L. 1980. See Solomon & Edmunds 1980, pp. 1–18

Blitz L. 1993. See Levy & Levine 1993, pp. 125–61

Bok BJ. 1934. *Harvard Circ. No. 384*. Cambridge, MA: Harvard Univ. Press

Bonnell IA, Bate MR, Clarke CJ, Pringle JE. 2001a. *MNRAS* 323:785–94

Bonnell IA, Bate MR, Clarke CJ, Pringle JE. 2001b. *MNRAS* 324:573–79

Bonnell IA, Bate MR, Zinnecker H. 1998. *MNRAS* 298:93–102

Bonnell IA, Davies MB. 1998. *MNRAS* 295:691–98

Bontemps S, Andre P, Kaas AA, Nordh L, Olofsson G, et al. 2001. *Astron. Astrophys.* 372:173–94

Bouvier J, Stauffer JR, Martin EL, Barrado y Navascues D, Wallace B, Bejar VJS. 1998. *Astron. Astrophys.* 336:490–502

Brandl B, Brandner W, Eisenhauer F, Moffat AFJ, Palla P, Zinnecker H. 1999. *Astron. Astrophys.* 352:L69–72

Brandner W, Zinnecker H, Alcala JM, Allard F, Covino E, et al. 2000. *Astron. J.* 120:950–62

Burrows A, Marley M, Hubbard WB, Lunine JI, Guillot T, et al. 1997. *Ap. J.* 491:856–75

Cambresy L, Beichman C, Cutri R. 2002. *Astron. J.* 123:2559–73

Carpenter JM. 2000. *Astron. J.* 120:3139–61

Carpenter JM, Heyer MH, Snell RL. 2000. *Ap. J. Suppl.* 130:381–402

Carpenter JM, Meyer MR, Dougados C,

Strom SE, Hillenbrand LA. 1997. *Astron. J.* 114:198–221
Carpenter JM, Snell RL, Schloerb FP. 1995. *Ap. J.* 450:201–16
Carpenter JM, Snell RL, Schloerb FP, Skrutskie MF. 1993. *Ap. J.* 407:657–79
Casali MM, Eiroa C. 1996. *Astron. Astrophys.* 306:427–35
Casali MM, Matthews HE. 1992. *MNRAS* 258:399–403
Chen Y, Zheng X-W, Yao Y, Yang J, Sato S. 2003. *Astron. Astrophys.* In press
Chini R, Kruegel E, Wargau WF. 1992. *Astron. Astrophys.* 265:45–54
Clarke CJ, Bonnell IA, Hillenbrand LA. 2000. See Mannings et al. 2000, pp. 151–77
Comeron F, Rieke GH, Burrows A, Rieke MJ. 1993. *Ap. J.* 416:185–203
Comeron F, Rieke GH, Rieke MJ. 1996. *Ap. J.* 473:294–303
D'Antona F, Mazzitelli I. 1994. *Ap. J. Suppl.* 90:467–500
D'Antona F, Mazzitelli I. 1997. *Mem. Soc. Astron. Ital.* 68:807
Davis CJ, Matthews HE, Ray TP, Dent WRF, Richer JS. 1999. *MNRAS* 309:141–52
de Grijs R, Johnson RA, Gilmore GF, Frayn CM. 2002. *MNRAS* 331:228–44
Dobbie PD, Pinfield DJ, Jameson RF, Hodgkin ST. 2002. *MNRAS* 335:L79–83
Duchene G. 1999. *Astron. Astrophys.* 341:547–52
Duchene G, Bouvier J, Simon T. 1999. *Astron. Astrophys.* 343:831–40
Dutra CM, Bica E. 2001. *Astron. Astrophys.* 376:434–40
Eiroa C, Casali MM. 1992. *Astron. Astrophys.* 262:468–82
Eisenhauer F, Quirrenbach H, Zinnecker H, Genzel R. 1998. *Ap. J.* 498:278–92
Elmegreen BG. 1991. See Lada & Kylafis 1991, pp. 35–60
Elmegreen BG. 1983. *MNRAS* 203:1011–20
Elmegreen BG, Clemens C. 1985. *Ap. J.* 294:523–32
Elmegreen BG, Efremov YN. 1997. *Ap. J.* 480:235–45
Elmegreen BG, Efremov Y, Pudritz RE, Zinnecker H. 2000. See Mannings et al. 2000, pp. 179–215
Fletcher A, Stahler S. 1994a. *Ap. J.* 435:313–28
Fletcher A, Stahler S. 1994b. *Ap. J.* 435:329–38
Geyer MP, Burkert A. 2001. *MNRAS* 323:988–94
Ghez AM, Neugegauer G, Matthews K. 1993. *Ap. J.* 106:2005
Gilmore G, Howell D. 1998. *The Initial Mass Function*. San Francisco: The Astron. Soc. Pac.
Giovannetti P, Caux E, Nadeau D, Monin J. 1998. *Astron. Astrophys.* 330:990–98
Goodwin SP. 1997. *MNRAS* 284:785–802
Grasdalen G, Strom SE, Strom KM. 1973. *Ap. J. Lett.* 184:L53–57
Greene TP, Lada CJ. 1996. *Astron. J.* 112:2184–221
Greene TP, Lada CJ. 1997. *Astron. J.* 114:2157–65
Greene TP, Lada CJ. 2002. *Astron. J.* 124:2185–93
Greene TP, Meyer MR. 1995. *Ap. J.* 450:233–44
Greene TP, Wilking BA, Andre P, Young ET, Lada CJ. 1994. *Ap. J.* 434:614–26
Haisch KE, Lada EA, Lada CJ. 2000. *Astron. J.* 120:1396–409
Haisch KE, Lada EA, Lada CJ. 2001a. *Ap. J. Lett.* 553:L153–56
Haisch KE, Lada EA, Lada CJ. 2001b. *Astron. J.* 121:2065–74
Haisch KE, Lada EA, Pina RK, Telesco CM, Lada CJ. 2001c. *Astron. J.* 121:1512–21
Hartmann L. 2001. *Astron. J.* 121:130–39
Hayashi C. 1966. *Annu. Rev. Astron. Astrophys.* 4:171–92
Herbig GH. 1998. *Ap. J.* 497:736–58
Herbig GH, Dahm SE. 2002. *Astron. J.* 123:304–27
Hillenbrand LA. 1997. *Astron. J.* 113:1733–68
Hillenbrand LA, Carpenter JM. 2000. *Ap. J.* 540:236–54
Hillenbrand LA, Hartmann L. 1998. *Ap. J.* 492:540–53
Hills JG. 1980. *Ap. J.* 240:242–45

Hodapp KW. 1994. *Ap. J. Suppl.* 94:615–49
Hodapp KW, Rayner J. 1991. *Astron. J.* 102: 1108–17
Horner DJ, Lada EA, Lada CJ. 1997. *Astron. J.* 113:1788–98
Howard EM, Pipher JL, Forrest WJ. 1997. *Ap. J.* 481:327–42
Hurt RL, Barsony M. 1996. *Ap. J. Lett.* 460:L45–48
Jiang ZB, Yao YQ, Yang J, Ando M, Kato D, et al. 2002. *Ap. J.* 577:245–59
Kenyon SJ, Gomez M. 2001. *Astron. J.* 121:2673–80
Kenyon SJ, Hartmann L. 1995. *Ap. J. Suppl.* 101:117–71
Kenyon SJ, Lada EA, Barsony M. 1998. *Astron. J.* 115:252–62
Klessen RS. 2001. *Ap. J.* 556:837–46
Klessen RS, Burkert A. 2000. *Ap. J. Suppl.* 128:287–319
Klessen RS, Burkert A. 2001. *Ap. J.* 549:386–401
Klessen RS, Heitsch F, Mac Low M-M. 2000. *Ap. J.* 535:887–906
Knee LBG, Sandell G. 2000. *Astron. Astrophys.* 361:671–84
Kramer C, Stutzki J, Rohrig R, Corneliussen U. 1998. *Astron. Astrophys.* 329:249–64
Kroupa P. 1995a. *MNRAS* 277:1491–506
Kroupa P. 1995b. *MNRAS* 277:1507–21
Kroupa P. 2002. *Science* 295:82–91
Kroupa P, Aarseth S, Hurley J. 2001. *MNRAS* 321:699–712
Kroupa P, Boily CM. 2002. *MNRAS* 336:1188–94
Kroupa P, Petr M, McCaughrean MJ. 1999. *New Astron.* 4:495–501
Kroupa P, Tout CA, Gilmore G. 1990. *MNRAS* 244:76–85
Kroupa P, Tout CA, Gilmore G. 1991. *MNRAS* 251:293–302
Kroupa P, Tout CA, Gilmore G. 1993. *MNRAS* 262:545–87
Lada CJ. 1987. In *Star Forming Regions, IAU Symp. No. 115*, ed. M Peimbert, J Jugaku, pp. 1–17. Dodrecht: Reidel
Lada CJ, Alves JF, Lada EA. 1996. *Astron. J.* 111:1964–76
Lada CJ, DePoy DL, Merrill KM, Gatley I. 1991. *Ap. J.* 374:533–39
Lada CJ, Kylafis ND, eds. 1991. *The Physics of Star Formation and Early Evolution*. Dodrecht: Kluwer. 746 pp.
Lada CJ, Kylafis ND, eds. 1999. *The Origin of Stars and Planetary Systems*. Dordrecht: Kluwer. 718 pp.
Lada CJ, Lada EA. 1991. In *The Formation and Evolution of Star Clusters*, ed. K Janes, pp. 3–22. San Francisco: Astron. Soc. Pac.
Lada CJ, Lada EA, Muench AA, Haisch KE, Alves J. 2002. In *The Origins of Stars and Planets: the VLT View*, ed. J Alves, M McCaughrean, pp. 155–70. Berlin: Springer-Verlag
Lada CJ, Margulis M, Dearborn D. 1984. *Ap. J.* 285:141–52
Lada CJ, Muench AA, Haisch KE, Lada EA, Alves JF, et al. 2001. *Ap. J.* 120:3162–76
Lada CJ, Wilking BA. 1984. *Ap. J.* 287:610–21
Lada CJ, Young ET, Greene T. 1993. *Ap. J.* 408:471–83
Lada EA. 1992. *Ap. J. Lett.* 393:L25–28
Lada EA. 1999. See Lada & Kylafis 1999, pp. 441–78
Lada EA, Bally J, Stark AA. 1991a. *Ap. J.* 368:432–44
Lada EA, DePoy DL, Evans JH, Gatley I. 1991b. *Ap. J.* 371:171–84
Lada EA, Evans NJ, Falgarone E. 1997. *Ap. J.* 488:286–306
Lada EA, Lada CJ. 1995. *Astron. J.* 109:1682–96
Lada EA, Lada CJ, Muench AA. 1998. In *The Initial Mass Function*, ed. G Gilmore, D Howell, pp. 107–20. San Francisco: Astron. Soc. Pac.
Lefloch B, Castets A, Cernicharo J, Langer WD, Zylka R. 1998. *Astron. Astrophys.* 334:269–79
Leinert Ch, Zinnecker H, Weitzel N, Christou J, Ridgeway ST, et al. 1993. *Astron. Astrophys.* 278:129–49
Leisawitz D, Bash FN, Thaddeus P. 1989. *Ap. J. Suppl.* 70:731–812
Levy EH, Levine JI, eds. 1993. *Protostars and*

Planets III. Tucson: Univ. Ariz. Press. 1596 pp.
Lissauer JJ. 2001. *Nature* 409:23
Lucas PW, Roche PF. 2000. *MNRAS* 314:858–64
Luhman KL. 1999. *Ap. J.* 525:466–81
Luhman KL. 2000. *Ap. J.* 544:1044–55
Luhman KL, Rieke GH, Lada CJ, Lada EA. 1998. *Ap. J.* 508:347–69
Luhman KL, Rieke GH, Young ET, Cotera AS, Chen H, et al. 2000. *Ap. J.* 540:1016–40
Lynden-Bell D, Pringle J. 1974. *MNRAS* 168:603–37
Lynga G. 1987. *Catalogue of Open Cluster Data*. Strasbourg, Fr.: Stellar Data Cent. Obs. Strasbourg. 5th ed.
Mannings V, Boss AP, Russell SS, eds. 2000. *Protostars and Planets IV*. Tucson: Univ. Ariz. Press. 1422 pp.
Marschall LA, van Altena WF, Chiu L-TG. 1982. *Astron. J.* 87:1497–506
Matzner CD, McKee CF. 2000. *Ap. J.* 545:364–78
McCaughrean MJ, Rayner JT, Zinnecker H. 1994. *Ap. J. Lett.* 436:L189–92
Megeath ST. 1996. *Astron. Astrophys.* 311:134–44
Megeath ST, Herter T, Beichman C, Gautier N, Hester JJ, et al. 1996. *Astron. Astrophys.* 307:775–90
Megeath ST, Wilson TL. 1997. *Astron. J.* 114:1106–26
Meyer MR, Adams FC, Hillenbrand LA, Carpenter J. 2000. See Mannings et al. 2000, pp. 121–49
Moitinho A, Alves J, Huelamo N, Lada CJ. 2001. *Ap. J. Lett.* 563:L73–76
Motte F, Andre P, Neri R. 1998. *Astron. Astrophys.* 336:150–72
Motte F, Andre P, Ward-Thompson D, Bontemps S. 2001. *Astron. Astrophys.* 372:41–44
Mouschovias TCh. 1991. *Ap. J.* 373:169–86
Muench AA, Alves JF, Lada CJ, Lada EA. 2001. *Ap. J. Lett.* 558:L51–54
Muench AA, Lada EA, Lada CJ. 2000. *Ap. J.* 553:338–71
Muench AA, Lada EA, Lada CJ, Alves JF. 2002. *Ap. J.* 573:366–93
Muench AA, Lada EA, Lada CJ, Elston RJ, Alves JF, et al. 2003. *Astron. J.* In press
Mundy LG, Looney LW, Lada EA. 1995. *Ap. J. Lett.* 452:L137–41
Myers PC. 1998. *Ap. J. Lett.* 496:L109–12
Najita J, Tiede GP, Carr JS. 2000. *Ap. J.* 541:977–1003
Natta A, Testi L. 2001. *Astron. Astrophys.* 367:L22–25
Natta A, Testi L, Comeron F, Oliva E, D'Antona E, et al. 2002. *Astron. Astrophys.* 393:597–609
Nurnberger DEA, Petr-Gotzens MG. 2002. *Astron. Astrophys.* 382:537–53
O'Connell DJK. 1957. *Stellar Populations*. Rome: Pontifical Acad. Sci. 522 pp.
Olmi L, Testi L. 2002. *Astron. Astrophys.* 392:1053–68
Oort J. 1957. See O'Connell 1957. pp. 507–16
Palla F, Stahler SW. 1999. *Ap. J.* 525:722–83
Palla F, Stahler SW. 2000a. *Ap. J.* 525:772–83
Palla F, Stahler SW. 2000b. *Ap. J.* 540:255–70
Park B-G, Sung H, Bessell MS, Kang YH. 2000. *Astron. J.* 120:894–908
Patience J, Duchene G. 2001. In *The Formation of Binary Stars, IAU Symp. No. 200*, ed. H Zinecker, R Mathieu, pp. 181–90. San Francisco: Astron. Soc. Pac.
Persi P, Roth M, Tapia M, Ferrari-Toniolo M, Marenzi AR. 1994. *Astron. Astrophys.* 282:474–84
Petr M, Du Foresto VC, Beckwith SVW, Richichi A, McCaughrean MJ. 1998. *Ap. J.* 500:825–37
Phelps R, Lada EA. 1997. *Ap. J.* 477:176–82
Piche F. 1993. *Publ. Astron. Soc. Pac.* 105:324–24
Prosser CF, Stauffer JR, Hartmann L, Soderblom DR, Jones BF, et al. 1994. *Ap. J.* 421:517
Reipurth B, Clarke C. 2001. *Astron. J.* 122:432–39
Rho J, Cocran MF, Chu YH, Reach WT. 2001. *Ap. J.* 562:446–55
Roberts MS. 1957. *Publ. Astron. Soc. Pac.* 69:59–64
Ruden S. 1999. See Lada & Kylafis 1999, pp. 643–79

Salpeter E. 1955. *Ap. J.* 121:161–67
Sandell G, Knee LBG. 2001. *Ap. J. Lett.* 546:L49–52
Santos CA, Yun JL, Clemens DP, Agostinho RJ. 2000. *Ap. J. Lett.* 540:L87–90
Scally A, Clarke C, McCaughrean MJ. 1999. *MNRAS* 306:253–56
Scalo JM. 1978. In *Protostars and Planets*, ed. T Gehrels, pp. 265–87. Tucson: Univ. Ariz. Press
Scalo JM. 1986. *Fund. Cosm. Phys.* 11:1–278
Schaller G, Schaerer D, Meynet G, Maeder A. 1992. *Astron. Astrophys.* 96:269
Seiss L, Dufour E, Forestini M. 2000. *Astron. Astrophys.* 358:593–612
Shu FH, Adams FC, Lizano S. 1987. *Annu. Rev. Astron. Astrophys.* 25:23–81
Simon M, Close LM, Beck TL. 1999. *Astron. J.* 117:1375–86
Simon M, Ghez AM, Leinert Ch, Cassar L, Chen WP, et al. 1995. *Ap. J.* 443:625–37
Sirianni M, Nota A, Leigherer C, De Marchi G, Clampin M. 2000. *Ap. J.* 533:203–14
Skrutskie MF, Dutkevitch D, Strom SE, Edwards SE, Strom KM, Shure MA. 1990. *Astron. J.* 99:1187–95
Solomon PM, Edmunds MG. 1980. *Giant Molecular Clouds in the Galaxy*. Oxford: Pergamon. 344 pp.
Spitzer L. 1958. *Ap. J.* 127:17–27
Strom KM, Strom SE, Edwards S, Cabrit S, Skrutskie MF. 1989. *Astron. J.* 97:1451–70
Strom KM, Strom SE, Merrill KM. 1993. *Ap. J.* 412:233–53
Strom SE, Edwards S, Skrutskie MF. 1993. See Levy & Levine 1993, pp. 837–44
Tapia M, Persi P, Roth M. 1996. *Astron. Astrophys.* 316:102–10
Testi L, Palla F, Natta A. 1998. *Astron. Astrophys.* 133:81–121
Testi L, Sargent AI. 1998. *Ap. J. Lett.* 508:L91–94
Thi WF, Blacke GA, von Dishoeck EF, van Zadelhoff GH, Horn JMM, et al. 2001. *Nature* 409:60
Trumpler RJ. 1931. *Publ. Astron. Soc. Pac.* 43:255–60
van den Ancker ME, The PS, Feinstein A, Vazquez RA, de Winter D, Perez MR. 1997. *Astron. Astrophys.* 123:63–82
van den Bergh S, Lafontaine A. 1984. *Astron. J.* 89:1822–24
van den Bergh S, McClure RD. 1980. *Astron. Astrophys.* 88:360–62
Veschueren W, David M. 1989. *Astron. Astrophys.* 219:105–20
Walker MF. 1956. *Ap. J. Suppl.* 2:365–87
Warin S, Castets A, Langer WD, Wilson RW, Pagani L. 1996. *Astron. Astrophys.* 306:935–46
Whitworth A. 1979. *MNRAS* 186:59–67
Wilking BA, Greene TP, Meyer MR. 1999. *Astron. J.* 117:469–82
Wilking BA, Lada CJ. 1983. *Ap. J.* 274:698–716
Wilking BA, Lada CJ, Young ET. 1989. *Ap. J.* 340:823–52
Wilking BA, McCaughrean MJ, Burton MG, Giblin T, Rayner JT, Zinnecker H. 1997. *Astron. J.* 114:2029–42
Wolf G, Lada CJ, Bally J. 1990. *Astron. J.* 100:1892–902
Wood K, Lada CJ, Bjorkman JE, Kenyon SJ, Whitney B, Wolff MJ. 2001. *Ap. J.* 567:1183–91
Zinnecker H, McCaughrean M, Wilking BA. 1993. See Levy & Levine 1993, pp. 429–95

Figure 1 Optical (*top*) and Infrared (*bottom*) images of the RCW 38 region obtained with the ESO VLT. The infrared observations reveal a rich embedded cluster otherwise invisible at optical wavelengths. Figure courtesy of J. Alves.

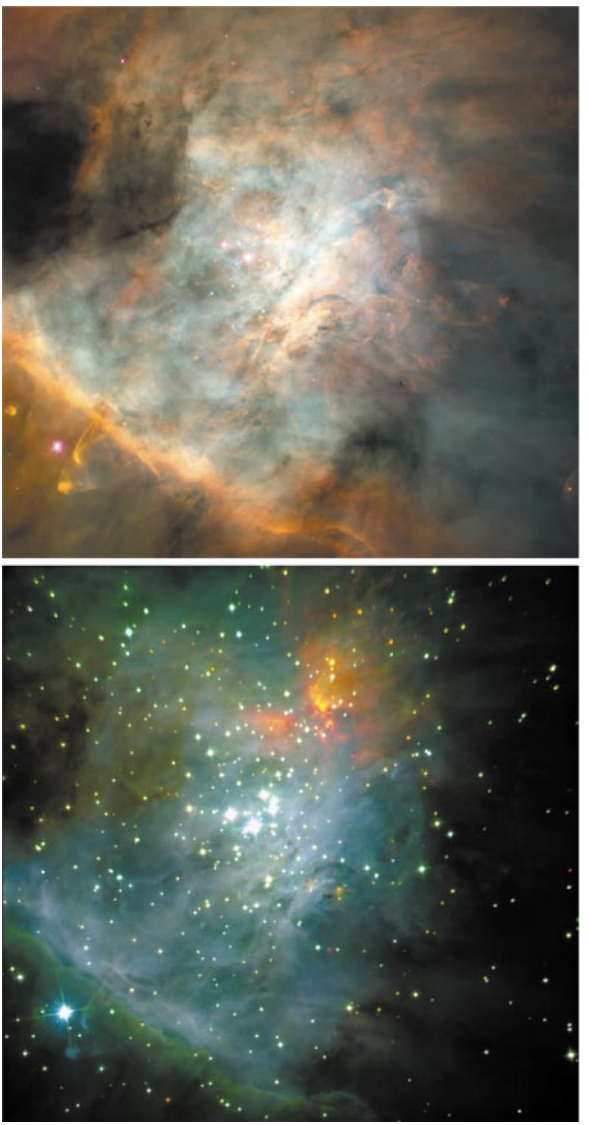

Figure 8 Optical (*top*) and deep *JHK* infrared (*bottom*) images of the Trapezium cluster in Orion obtained with the NASA *HST* and the ESO Very Large Telescope, respectively. The infrared observations taken from Muench et al. 2002.

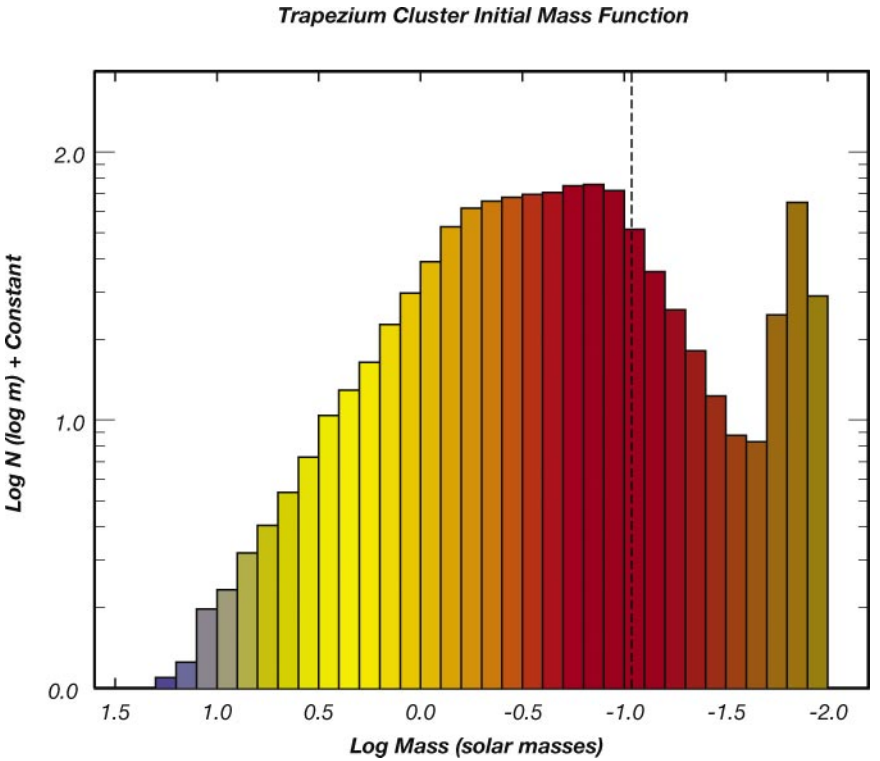

Figure 10 The IMF derived for the Trapezium cluster from Monte Carlo modeling of its luminosity function (Muench et al. 2002). This plot displays the binned mass function of the synthetic cluster whose luminosity function was found to best fit the observed KLF of the Trapezium cluster (see Figure 9). A vertical dashed line marks the approximate location of the hydrogen burning limit (HBL). The derived IMF displays a broad peak between 0.1–0.6 $M_{\odot}$ and extends deep into the substellar mass regime. The secondary peak is located near 0.015 $M_{\odot}$ or 15 M_{J}. It corresponds to the bump in the KLF at K ~ 15.5 magnitudes seen in Figure 9 and may be an artifact of the adopted substellar MLR.

Figure 16 Deep wide-field, infrared image of the extremely young protocluster associated with NGC 1333. The cluster is deeply buried in a massive molecular cloud core. Numerous outflows and jets are visible in the image. These have been generated by embedded protostellar objects and have significantly modified the structure of the massive molecular core. Image was obtained with the University of Florida wide-field imager and multi-object spectrometer.